



THE EARTH OBSERVER

November / December 2004, Vol. 16, No. 6

In this issue ...

Meeting/Workshop Summaries

SORCE Science Meeting.....	3
Aqua Science Working Group.....	17

Other Items of Interest

Pathfinding for EOS Product Data Format Transition from HDF-EOS2 to HDF-EOS5.....	33
Kudos.....	2, 32, 38
AMSR-E SIPS Historical Processing Completed.....	38

Regular Features

Earth Science Education Program Up- date.....	39
EOS Scientists in the News.....	42
Science Calendars.....	43
The Earth Observer Information/ Inquiries.....	Back Cover

EDITOR'S CORNER

Michael King

EOS Senior Project Scientist

I'm pleased to report that Congress has approved the Omnibus Appropriations Act for fiscal year 2005 (FY 2005), which encompassed nine separate spending bills that had not been passed before the election. The bill contains funding for the National Institutes of Health (NIH), the National Science Foundation (NSF), the National Oceanic and Atmospheric Administration (NOAA), National Aeronautics and Space Administration (NASA), the Office of Science within the Department of Energy (DOE), the Department of Education (ED), and numerous other federal agencies.

The Omnibus Appropriations Act included \$16.2 billion for NASA in FY 2005. This funding is \$822 million above the FY 2004 level, but \$44 million below the President's request. These figures and the ones below do not include the 0.8% across the board reduction to be applied to NASA programs as the agency's operating plan is developed. NASA's new vision maps out an aggressive role for the United States in both manned and unmanned space exploration. The Shuttle program and the construction of the International Space Station (ISS) continue to be the primary focus of the Nation's manned space flight activities.

NASA requested and the conferees provided "unrestrained transfer authority between the Exploration Capabilities account and the Science, Aeronautics, and Exploration account." Though this gives NASA significant control over its own budget, NASA is obligated to report back to Congress within a 60-day period to account for any alterations to program values. This flexibility will allow NASA to cover the increasing costs of the servicing mission for the Hubble Space Telescope that is already appropriated at \$291 million, but expected to cost more, as well as return-to-flight activity. However, this transfer flexibility could also increase vulnerability for science programs as NASA grapples with the funding needed for Space Station, the Moon-Mars mission, and other exploration programs.

Continued on page 2

With regard to NASA's Earth Science activities, the Earth Science Applications Program is funded at \$15 million above the President's request for competitively selected projects. House and Senate negotiators continued to support the Earth Observing System Data and Information System (EOSDIS) Core System (ECS)/EOSDIS Maintenance and Development (EMD) Synergy Program with \$15 million for Synergy and \$12 million through the EOSDIS Maintenance and Development Contract to support an extension of the Synergy Data Pools to improve data distribution to climate change models. In addition to these allocations, \$5 million has been provided to update the NASA Center for Computational Science (NCCS) at Goddard Space Flight Center to operate as a backup to protect NASA from computer failure. The Office of Earth Science received \$56.3 million for numerous special projects.

Despite the transformation of NASA, the legislation directs NASA to, "remain, fully committed to Earth science, with future missions identified with a 5-year funding process that reflects a serious commitment to Earth Science as a vital part of the Nation's space program." The bill also includes supporting building the Aerosol

Polarimeter Sensor (APS) and Total Irradiance Monitor (TIM) instruments, but full budget support for the Glory Global Climate Change research program mission is not yet assured.

In other news, I would like to congratulate the French Space Agency—Centre Nationale d'Etudes Spatiale (CNES)—for the successful launch of the Polarization and Anisotropy of Reflectances for Atmospheric Science coupled with observations from a Lidar (PARASOL) mission on December 21, 2004, from the Guiana Space Center in Kourou, French Guiana aboard an Ariane 5 rocket. PARASOL will make measurements of the total polarized light in several wavelengths and at several different viewing angles, and should help scientists better characterize clouds and aerosols in the atmosphere, including determining how much of the aerosol present is the result of human activities. PARASOL joins Aqua and Aura (already in orbit) as part of the Afternoon Satellite Constellation (A-Train). When complete the formation will also include CloudSat, Cloud-Aerosol Lidar and Infrared Pathfinder Satellite Observations (CALIPSO), and the Orbiting Carbon Observatory (OCO). The combination of observations made possible by this forma-

tion of satellites, each flying in very close proximity to one another, offers an unprecedented resource for exploring aerosol-chemistry-cloud interactions and how each of these impact Earth's climate.

CloudSat and CALIPSO are scheduled to join the A-Train later this year. A joint launch is currently planned for no earlier than July 5, 2005. The powerful Cloud Profiling Radar on CloudSat will allow for the most detailed study of clouds to date. Meanwhile, CALIPSO will carry a lidar called Cloud Aerosol Lidar with Orthogonal Projection (CALIOP), and also carries two passive imagers—a three-channel Infrared Imaging Radiometer (IIR), and a Wide-Field Camera (WFC) that acquires visible images. The measurements acquired by CloudSat and CALIPSO should improve our understanding of the role aerosols and clouds play in regulating Earth's climate.

Finally, I would like to acknowledge the fifth anniversary of the Terra mission. Terra served as the flagship of the Earth Observing System (EOS) and continues to bring back outstanding science data. I would like to congratulate everyone who has been part of this highly successful mission.



Kudos

NASA and the U.S. Department of Interior recently presented The William T. Pecora Award for excellence in remote sensing to **William Krabill**, NASA Wallops Flight Facility, VA.

Krabill is an investigator for airborne lidar topographic mapping and Global Position System (GPS) applications. His vision of combining airborne laser-ranging measurements and GPS has revolutionized glaciology, coastal-zone mapping and measurement of land-surface change.

The William T. Pecora Award is presented annually to individuals or groups that make outstanding contributions in the field of remote sensing and its application to understanding the Earth.

The Earth Observer staff and the EOS scientific community congratulate Krabill on this outstanding accomplishment.

SORCE Science Meeting Addresses “Decadal Variability in the Sun and Climate”

— Judith Lean, jlean@ssd5.nrl.navy.mil, Naval Research Laboratory
 — Greg Kopp, kopp@lasp.colorado.edu, Laboratory for Atmospheric and Space Physics, University of Colorado
 — Mark Baldwin, mark@nwra.com, Northwest Research Associates
 — Gary Rottman, gary.rottman@lasp.colorado.edu, Laboratory for Atmospheric and Space Physics, University of Colorado
 — David Rind, drind@giss.nasa.gov, Goddard Institute for Space Studies, Columbia University
 — Peter Pilewskie, peter.pilewskie@lasp.colorado.edu, University of Colorado
 — Tom Woods, woods@lasp.colorado.edu, Laboratory for Atmospheric and Space Physics, University of Colorado
 — Robert Cahalan, robert.cahalan@gssc.nasa.gov, NASA Goddard Space Flight Center

After 18 extremely successful months in orbit, the Solar Radiation and Climate Experiment (SORCE) continues to engage the scientific community. EOS’s SORCE mission is measuring the Sun’s total and spectral irradiance with unprecedented accuracy and spectral coverage. SORCE data are providing new information to the science community to address solar variability relating to climate effects and potential climate response mechanisms. The SORCE program is fostering a unique venue for ongoing scientific exchange about the Sun and climate.

The SORCE team and interested scientists recently met in Meredith, New Hampshire to discuss *Decadal Variability in the Sun and Climate*. Approximately 75 people attended the meeting held October 27-29, 2004. The meeting was an opportunity to further understand the evidence for, and mechanisms involved in, decadal variability in the Sun and climate, with emphasis on their possible connections.

Discerning the role of the Sun in climate variations on time scales of decades is a challenging task. It is now relatively well established that climate forcing is well correlated with total irradiance and UV irradiance measurements obtained from high-precision

space-based solar measurements spanning more than two decades. When the Sun is near the maximum of its activity cycle, it is about 0.1% brighter overall, with an order of magnitude greater increase at UV wavelengths. SORCE measures these variations with unprecedented accuracy, precision, and spectral coverage across the UV, visible, and IR. But how—and if—climate responds to these measured solar variations presents a major puzzle. The meeting sessions focused on detecting and understanding plausible mechanisms both through direct surface heating and indirectly through the stratosphere.

Widespread empirical evidence from the extensive Earth climate data sets suggests the presence of an 11-year solar signal on the order 0.1 K in surface, atmospheric, and ocean temperatures. But general circulation models (GCMs) underestimate this response by as much as a factor of five. The GCMs account primarily for direct forcing by changing incoming total radiation and assume that the response time for climate feedback processes to this external forcing is on the order of 100 years. Processes and pathways not included in the GCMs may help facilitate the larger than predicted climate response to decadal solar variability. Solar variations in the UV spectrum modulate

stratospheric ozone concentrations, which may couple to climate via radiative and dynamical pathways. These pathways may involve the Northern and Southern annular modes, allowing a solar signal to be amplified and reach Earth’s surface. Internal atmosphere-ocean oscillations such as the North Atlantic Oscillation (NAO) and the El Niño Southern Oscillation (ENSO) may also play a role. Clouds may expedite the feedback process, as they appear to also exhibit variability with the solar cycle. Stochastic climate variability may amplify the relatively small solar variations. Other, non-linear, climate processes are speculated.

With almost 60 abstracts submitted, attendees enthusiastically shared information, ideas, and opinions over the two-and-one-half days of oral and poster presentations. Most of the presentations are available on the SORCE Meeting website at: lasp.colorado.edu/sorce/2004ScienceMeeting/Meeting_Review.html.

The scientific organizing committee, **Mark Baldwin** from Northwest Research Associates, **Greg Kopp** from the Laboratory for Atmospheric and Space Physics (LASP), and **Judith Lean** from NRL, arranged the meeting into four sessions:

1. Solar Radiation—Status of Current
SORCE Measurements
2. Decadal Variability in the Atmo-
sphere and Oceans
3. Mechanisms and Modes of Decadal
Solar Variability
4. Climate Variability Modes, e.g.,
ENSO, NAO/ Arctic Oscillation
(AO), Pacific Decadal Oscillation
(PDO) and Nonlinear Response

An invited keynote speaker began each day with a thoughtful and enlightening overview talk, and meeting attendees enjoyed a provocative science dinner lecture.

Keynote Talks

Meeting Chair, **Mark Baldwin** (Northwest Research Associates, Bellevue, Washington) began the meeting with a tutorial on *The Stratospheric Link Between the Sun and Climate*. He intro-

duced the main Earth atmospheric modes such as the Quasi-Biennial Oscillation (QBO) and AO and discussed possible mechanisms whereby changes to the circulation of the lower stratosphere can affect surface climate. Possible stratospheric polar-vortex sensitivity to solar forcing may provide an indirect mechanism for climate change due to solar variability (see **Figure 1**).

On Thursday morning, **Vikram Mehta** (The Center for Research on the Changing Earth System, Columbia, Maryland) spoke on *“Decadal Climate Variability: Societal Impacts, Phenomena, Problems, and Prospects.”* He provided fascinating anecdotal evidence of how decadal and multi-decadal climate variability has influenced societies throughout history by affecting localized rainfall, fires, drought, fish catch, and hurricanes. But he noted that current climate predictions are not very accurate, partly due

to a limited time range of high-quality data. Mehta considered how the results would be used by society if climate variability prediction were reliable. Meeting attendees also learned about the Center for Research on the Changing Earth System (www.crces.org) for which decadal-to-century-scale climate variability is a special focus.

Madeleine Nash (*TIME* magazine contributor and book author, San Francisco, California) was a special guest at the meeting. She brought a new perspective to the SORCE Meeting on Friday morning when she presented *Chasing El Niño: A Science Writer’s Walk on the Wild Side of Climate*. She discussed the effects the 1997-98 El Niño had on individual societies and people (a topic she explores in her recent book, *El Niño: Unlocking the Secrets of the Master Weather-Maker*), and speculated about the effects that long-term climate change might have on societies collectively over the next century. Her insightful comparisons of the characteristics of scientists and journalists proved especially interesting. The science-based audience had several questions on improving interactions with the public, and a lively discussion ensued.

Session 1—Solar Radiation—Status of Current SORCE Measurements
Chair: Robert Cahalan (NASA Goddard Space Flight Center)

Gary Rottman, SORCE Principal Investigator, commenced Session 1 with an overview of the SORCE mission (see **Figure 2**). He reported that SORCE is in excellent health and providing daily total solar irradiance (TSI) and solar spectral irradiance data from the soft X-rays, through the ultraviolet, visible, and into the infrared. All aspects of the

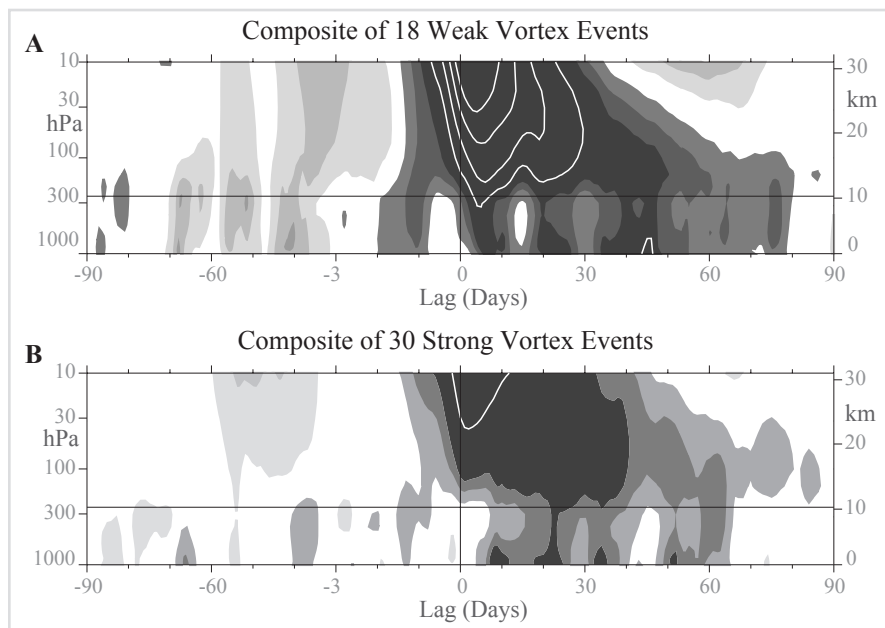
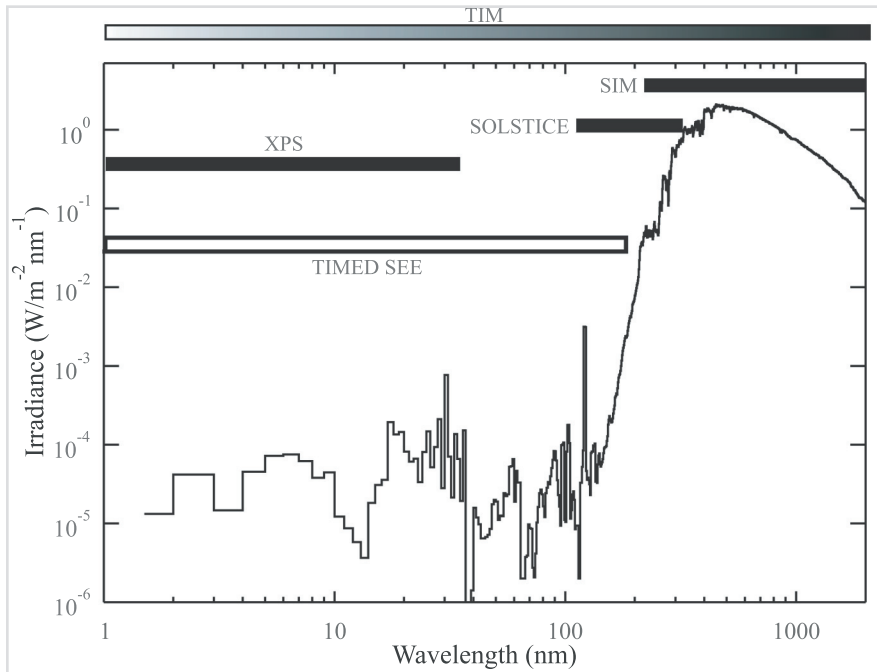


Figure 1: Composites of time-height development of the northern annular mode for (A) 18 weak vortex events and (B) 30 strong vortex events. The events are determined by the dates on which the 10-hPa annular-mode values cross -3.0 and +1.5, respectively. The indices are nondimensional; the contour interval for the shading is 0.25 and 0.5 for the contours. Values between -0.25 and 0.25 are unshaded. The thin horizontal lines indicate the approximate boundary between the troposphere and the stratosphere. (Baldwin, M.P and T.J. Dunkerton, Stratospheric Harbingers of Anomalous Weather Regimes, *Science*, 244, 581-584, 2001)

Figure 2: SORCE instruments and their wavelength coverage. (Gary Rottman)



mission exceed expectations with the spacecraft and instruments continuing to function flawlessly. Rottman concluded by stressing how very important it is to Sun-climate science to ensure the continuity of the solar data sets.

Following an introduction by Session Chair **Bob Cahalan**, each of the SORCE instrument scientists presented results from the first 18 months of the SORCE mission. A special focus was the observations of the dramatic flare, of almost unprecedented strength (in the space era) that occurred during the intense solar storm in October-November 2003 (shown in **Figure 3**). SORCE instruments are also providing excellent characterizations of solar rotational variability, which modulates the entire solar spectrum, and underlies the rapid surges of brightening seen during flares. As the SORCE mission continues, the instrument scientists expect to see reduced rotational modulation because solar activity is

declining. There is high anticipation that SORCE will eventually be able to characterize the Sun's 11-year cycle in irradiance at all wavelengths.

The Total Irradiance Monitor (TIM) instrument on SORCE measures total solar irradiance, continuing a database that extends without interruption back to 1978. **Greg Kopp** (LASP, University of Colorado) discussed the TIM results (see **Figure 3**). A crucial radiometric development is the offset of about -4 W/m^2 in the TIM absolute solar-irradiance value, as compared with other TSI measurements. After careful examination of all TIM calibration parameters and re-evaluation of data-processing algorithms, the SORCE scientists are now confident the new, lower values are correct. NASA and NIST calibration experts will convene a workshop(s) to address the differences between the various data sets, and hopefully in early 2005, a recommendation can be made to the climate community. *If solar irradiance is as low as 1361 W/m^2 , rather than the currently accepted value of 1365.5 W/m^2 , climate models may need revising.* TIM's beautiful observations of the

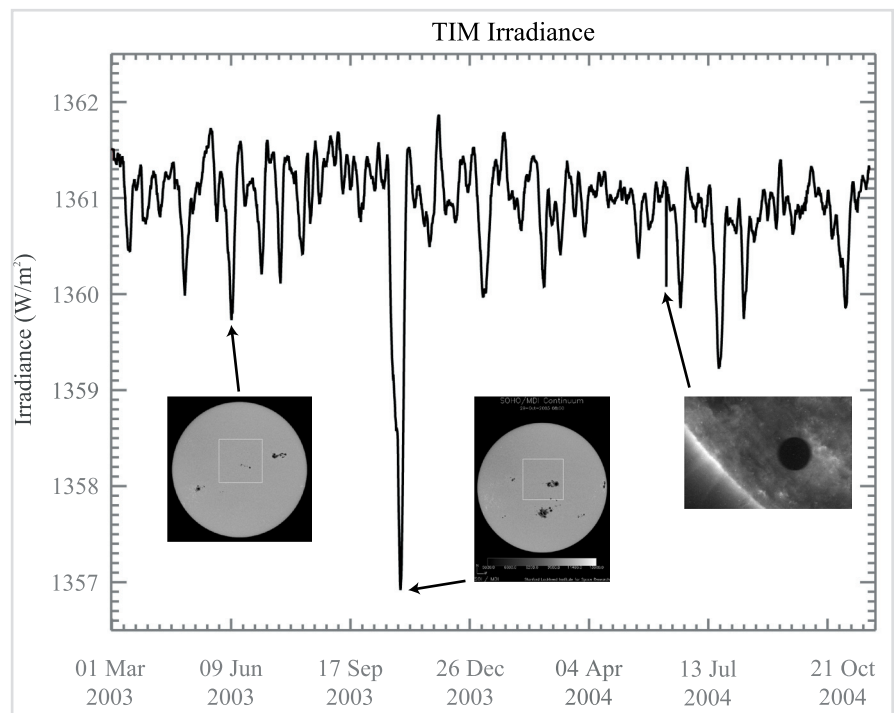


Figure 3: Over the life of the SORCE mission to date, the TIM has recorded the largest short-term decrease in TSI since space-borne measurements began, and has observed the transit of Venus across the Sun. (Greg Kopp)

Venus transit are exciting *serendipitous science*.

SORCE has a unique new capability to make precise measurements of spectral-irradiance variations that compose the changes in total irradiance. SORCE's Spectral Irradiance Monitor (SIM) is observing fluctuations in the entire solar spectrum from 0.2-2 μm . SIM instrument scientist, **Jerry Harder** (LASP, University of Colorado) reviewed the visible and near-infrared results. Harder pointed out important differences between the SIM measurements and models of solar spectral-irradiance variability that various climate model studies have used. He emphasized the need to refine solar models in the infrared region. He concluded that solar images, TSI, and solar modeling in conjunction with SIM spectral irradiance measurements provide an effective and unprecedented suite of research tools to investigate solar variability and achieve new understanding of its nature and causes.

Discussing the ultraviolet results from the Solar Stellar Irradiance Comparison Experiment (SOLSTICE) instrument, **Bill McClintock** (LASP, University of Colorado) presented new information about solar variability evident in the Magnesium-II (Mg II) core-to-wing index. SORCE SOLSTICE data continue to validate and refine the UV spectral-irradiance observations made by SOLSTICE on the Upper Atmosphere Research Satellite (UARS). Achieving a long-term database of high-quality solar UV irradiance is crucial for clarifying solar influences on ozone concentrations, and possible stratospheric forcing of climate. Like TIM, SOLSTICE is also providing exciting *serendipitous science*, including occultation measurements of ozone and molecular oxygen,

and lunar observations that suggest a lower lunar UV albedo (reflectivity) than previously thought.

The soft X-ray results from the Extreme Ultraviolet (XUV) Photometer System (XPS) instrument were covered by **Tom Woods**, LASP's SORCE Project Scientist. Woods talked about the latest XPS calibrations and additional flare measurements in June 2003 and July 2004. Woods' instruments on the simultaneously operating Thermosphere Ionosphere Mesosphere Energetics and Dynamics (TIMED) mission combine with the SORCE XPS to extend the spectral-irradiance coverage of SIM to the XUV region.

All SORCE science data are processed, analyzed, validated, and distributed through LASP's Mission and Science Operations Center in Boulder, Colorado. Processed data are distributed to the science community through the Goddard Earth Sciences (GES) Distributed Active Archive Center (DAAC). For additional information on obtaining SORCE data from the DAAC and reading the SORCE HDF data files, see: lasp.colorado.edu/sorce/data_access.html.

Session 2—Decadal Variability in the Atmosphere and Oceans

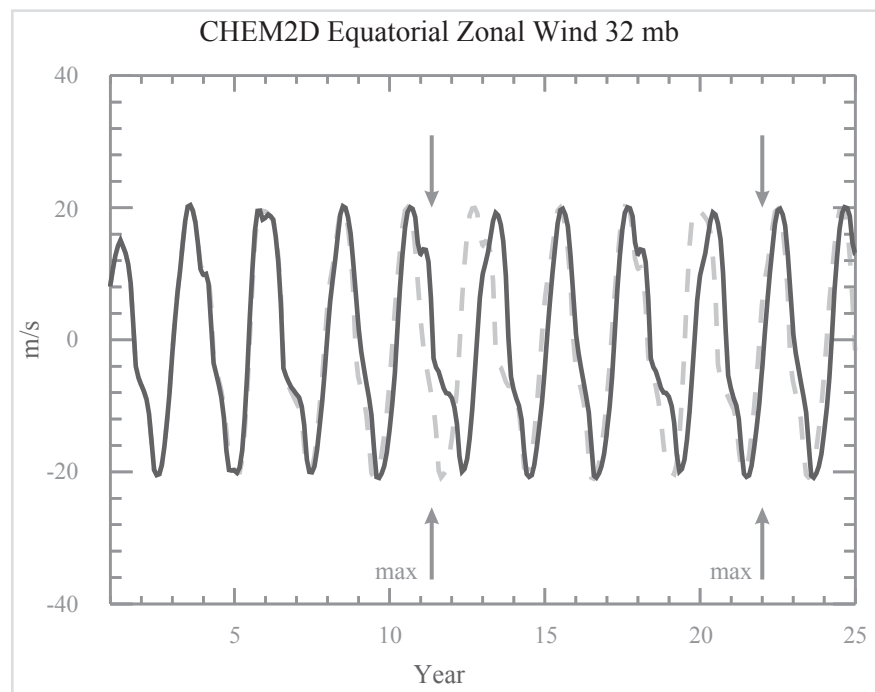
Chair: David Rind (Goddard Institute for Space Studies, Columbia University)

Session 2, chaired by climate-change expert **David Rind**, examined evidence for decadal variability in the Earth's atmosphere, with emphasis on exactly how solar-cycle effects might influence the stratosphere and troposphere. This is a continuing source of interest to the Sun-climate community, motivated by recent studies that appear to demonstrate a possible stratospheric influence

on climate. The direct solar heating in the stratosphere is becoming better observed, and a response is also detectable in the troposphere. The solar-cycle impact on the stratospheric circulation is increasingly seen as an interaction between the solar cycle, ozone, QBO, and the semi-annual oscillation (SAO) (which Mark Baldwin described in his keynote talk) in complicated ways, usually involving planetary-wave interactions. The effect on tropospheric dynamics may also involve synoptic-scale waves, although tropospheric responses are typically determined to be quite small.

Discussing empirical detection of the 11-year cycle as derived from observations of the lower troposphere, **David Douglass** (University of Rochester, NY) shared his findings of a solar-cycle-related temperature change of order 0.1°C . From this he inferred a climate sensitivity of $0.1^\circ\text{C}/\text{W}/\text{m}^2$, with a lower sensitivity to the seasonal variation in solar irradiance ($0.03\text{ C}/\text{W}/\text{m}^2$). Both sensitivities are much lower than GCMs produce and seem to imply a negative feedback relative to the decadal cycle. He combined the observations with the observation (now-disputed) that Microwave Sounding Unit (MSU) sensors show a cooling in the upper troposphere—in contrast to GCM-produced warming—to conclude that GCMs have inappropriate positive feedbacks and long response times. However, the sensitivity of the system depends on the time-scale of the forcing. The decadal cycle of five years up and five years down is too quick to incite most of the ocean warming and water vapor response. This is even more true of the seasonal cycle, which has an even lower sensitivity than the decadal cycle. Thus the full feedback response

Figure 4: When solar UV variations are included (dotted line), westerly QBO phase tends to be shorter near solar maximum (arrows). This effect is only present when zonal wind SAO is also included. (John McCormack)



requires consistent forcing lasting longer than a decade.

Particularly exciting are new developments in the detection and interpretation of solar signals in high-quality atmospheric databases that have existed for many decades. **Joanna Haigh** (Imperial College, London, UK), a leader in this area of work, presented her results from the National Centers for Environmental Prediction/National Center for Atmospheric Research (NCEP/NCAR) data. She related changes in the solar cycle to changes in the tropospheric zonal wind field, both in NCEP/NCAR observations and in a GCM. In both model and observations the subtropical tropospheric jets moved poleward as solar activity increased, although the model effects were somewhat smaller. The model response was related to a change in tropical upwelling and Hadley Cell strength (the Hadley Cell weakened and expanded poleward). To

investigate the mechanism involved, heating was added to a simplified GCM, changing the stratospheric temperatures at various latitudes. Uniform or high-latitude warming weakened the jets and moved them equatorward, while tropical warming produced changes in accord with the observations. The warming of the lower stratosphere affected the height of the tropopause, and the life cycle of baroclinic waves, explaining part of the response. While the variations involved are small—changes in the jet of 1 m/s—they are detectable at the 95% confidence level in the observations.

There is emerging evidence, both from analysis and modeling, that solar variability can influence the Earth's atmosphere by affecting its various modes of variability. **John McCormack** (Naval Research Laboratory [NRL], Washington, DC) discussed the relationship of the solar cycle to the QBO (and SAO).

Of particular interest was uncertainty as to the altitude at which the main interactions occur—in the lower stratosphere or the upper stratosphere. McCormack used the NRL CHEM2D model with full chemistry, a lower boundary forcing of the QBO, and the SAO forced by gravity-wave drag, to investigate possible interactions. His results are shown in **Figure 4**. The QBO was found to increase the variation in zonal wind from solar maximum to solar minimum by a factor of two (although it was still 2.5-times too weak). A shorter-phase westerly QBO at solar maximum in the model was found to be due to the SAO (although the difference in phase was less than half the observed). The conclusion was that both the QBO and SAO are needed and both altitudes are important. One problem is that the model (like others) was not able to reproduce in detail the observed variation of ozone with the solar cycle (model values have smaller amplitude changes and peak at lower altitudes). McCormack also noted that the Halogen Occultation Experiment (HALOE) observations don't seem to indicate the same ozone/solar-cycle effects as had been previously observed, underscoring an issue that would emerge again during the meeting—namely our relatively poor understanding of the solar-cycle variation of ozone.

To investigate the variability of the winter stratosphere with respect to the solar cycle, **Lesley Gray** (Reading University, UK) examined the last 20 years of the European Centre for Medium-Range Weather Forecasts (ECMWF) reanalysis (ERA-40). A multiple-regression analysis was performed with respect to the solar cycle (10.7 cm flux), volcanic aerosols, the NAO, ENSO, and the QBO. As **Figure 5** shows, a clear solar cycle is observable in temperature,

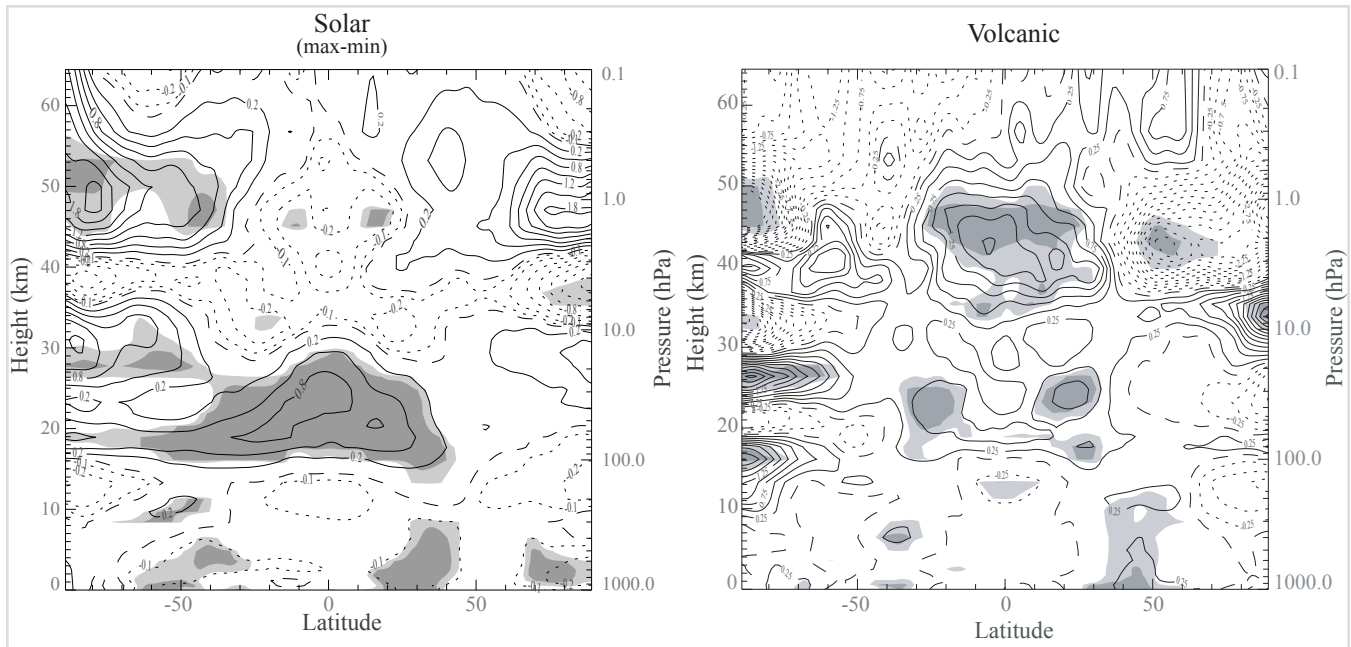


Figure 5: Latitude - height distribution of the zonally-averaged, annual-average amplitude of the 11-year solar cycle and volcanic signal in temperature (K) from a multiple regression analysis of the ERA-40 dataset for the period 1979–2001 (S. Crooks and L.J. Gray, *J. Clim.*, 2005, in press). The other components in the multiple regression included a long-term trend, seasonal variations, and representations of the NAO, ENSO and QBO.

on the order of 2 K at 40–50 km, with a secondary maximum at 20–25 km in the subtropics (in agreement with observations of Labitzke and van Loon). A zonal-wind response, of up to 6 m/s was found peaking at 50–60 km in the subtropics. This anomaly was associated with a tendency for stratospheric warmings to occur earlier with the east phase of the QBO and solar-minimum conditions. It was reproduced in a simple model, in which subtropical easterlies were pulled in around the polar vortex and used to build up the Aleutian High, leading to the earlier breakdown of the vortex. For this to happen, the anticyclones had to be coherent with depth, which means it also depends on the phase of the SAO. Hence both this and the previous talk emphasized the interaction of the solar cycle with oscillations throughout the depth of the stratosphere.

An understanding of the response of stratospheric ozone to changes in solar UV radiation is crucial for quantifying

mechanisms to explain the results presented by both Joanna Haigh and Lesley Gray. **Terry Nathan** (University of California, Davis) focused on how solar-cycle-induced perturbations to stratospheric ozone could impact the vertical propagation and downward reflection of forced planetary waves—a topic also discussed later in the meeting by his colleague Eugene Cordero. Nathan used a mechanistic (quasi-geostrophic) model of the extratropical atmosphere to account for the interactions between ozone, radiation, and dynamics. The results indicated that solar-cycle-induced ozone perturbations could change the refractive index of the planetary waves via two mechanisms: 1) by changes in the zonal-mean temperature gradient, which affects the zonal-mean wind via thermal-wind balance; and 2) by changes in the diabatic heating associated with wave-ozone interactions. The former mechanism has been considered in previous studies and represents an incomplete picture of how the solar cycle might af-

fect planetary wave reflection. The latter mechanism has not been considered before and represents a new pathway for communicating solar-cycle-induced changes in ozone heating to the lower atmosphere. Indeed, the second mechanism produces changes in the refractive index that cause the planetary waves to reflect downward into the troposphere where the poleward heat fluxes are altered.

Also focusing on wave motions, using a 2-level baroclinic model, **Alfred Powell** (NOAA/NESDIS/Office of Research Applications [ORA], Camp Springs, MD) investigated how the solar cycle might alter the planetary-wave spectrum. The basic idea is that static stability is changed during the solar cycle, and the critical wavelength for instability is affected by the static stability. In addition, as the temperature gradient is altered during the solar cycle, so is the vertical shear of the zonal wind, which also affects instability. The results showed that there was more energy at

solar maximum for short waves, and more energy during solar minimum for long waves, a combination of shear and static stability influence. The response also differed as a function of month. Overall, the change in energy was greatest during the maximum gradient of the solar flux. The conclusion was that both synoptic-scale and planetary-scale wave generation can be affected by solar-cycle influences, although it was estimated that the resulting changes were small (on the order of 3%).

Session 3—Mechanisms and Modes of Decadal Solar Variability

Chair: Stephen Walton (San Fernando Observatory, California State University)

A primary cause of solar-irradiance variations is the occurrence of bright active regions, called *faculae* (Latin for *torch*) on the Sun's disk. In fact, during the solar activity cycle, facular brightening dominates—by a factor of two—the darkening by sunspots to cause overall total-irradiance brightening at cycle maxima. Faculae have lower contrasts, are more spatially dispersed, and are not nearly as well understood as sunspots. Session 3 focused on recent research into solar mechanisms that cause variations in the Sun's output on decadal time scales, with particular emphasis on observations and models of faculae.

Commencing the session, **Dick White** (LASP, University of Colorado) examined current knowledge of the Sun's radiative output, based on measurements of various proxies of activity—the F10.7, Mg II, and sunspots—in relation to the rapid increase in global temperature over the last 50 years. He stressed the importance of the last 30 years specifically in measuring and understanding the total- and spectral-ir-

radiance variations, and for comparing solar variability to the Earth's global temperature. The current solar cycle 23 is an important case study. Whereas the prior solar activity cycles (numbers 21 and 22) were comparable in the strength of their activity (as indicated by similar sunspot numbers), cycle 23 is of overall lower activity. Facular indices such as the Mg II core-to-wing ratios don't appear to follow the sunspot numbers as well as they did in prior solar cycles, and TSI is comparable in the three cycles. Like many others, White concluded that solar-output changes cannot account for the rapid increase in global warming.

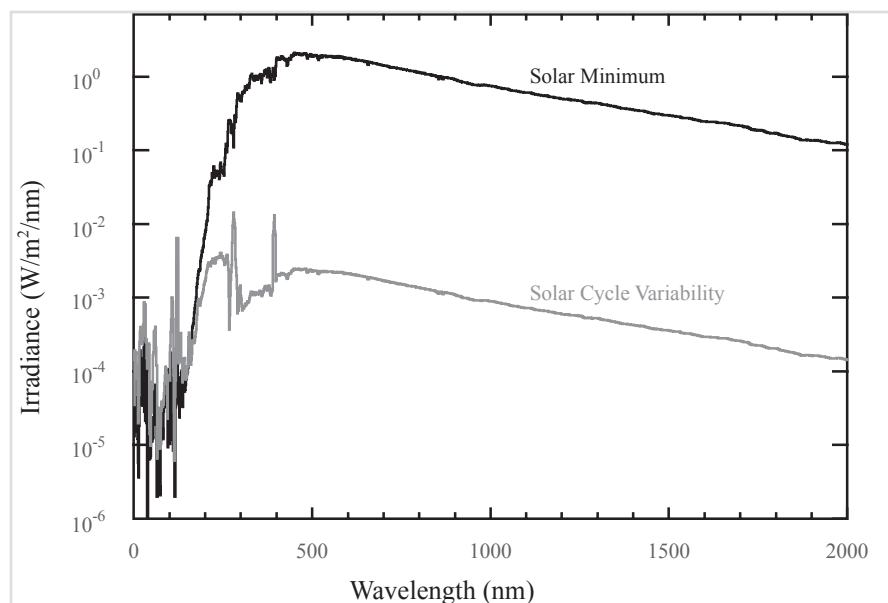
The San Fernando Observatory (SFO) has been making 5x5" full-disk photometric images in 3 wavelength bands since 1985 with higher resolution images and additional wavelength bands starting in 1992. Analysis of these images helps in understanding the sunspot and facular influences on TSI. **Stephen Walton** (San Fernando Observatory, California State University, Northridge) explained how daily photometric sums are computed, with contributions from high-relative-intensity pixels attributable to faculae and low-intensity pixels to sunspots. These sums correlate well with spacecraft measurements of TSI. He finds no solar-cycle variation in the broadband photometric sum in the *red* region of the solar spectrum. This suggests that visible-wavelength continuum radiation has no solar-cycle component, and that changes in the line blanketing by the solar atmosphere dominate the solar-cycle change in TSI. The SFO results also show that solar features larger than 10^{-4} of the solar hemisphere account for the majority (80%) of the solar-cycle variations in irradiance. Particularly interesting were Walton's preliminary comparisons of

the SFO image on September 1, 2003 converted to *bolometric* brightness maps (thus mimicking TSI) with new images that measure this quantity directly using the Solar Bolometric Imager, which Peter Foukal discussed later in the session.

Following from the 2002 SORCE meeting, in which there was considerable discussion of the constructions of composite records of TSI, **Claus Fröhlich** (Physikalisch-Meteorologisches Observatorium Davos, World Radiation Center, Switzerland) reported on his refined TSI composite. Fröhlich's composite now includes a re-analysis of: 1) the Solar Maximum Mission/Active Cavity Radiometer Irradiance Monitor (SMM/ACRIM-I) observations for an early sensitivity increase; and 2) the degradation of the Hickey-Frieden radiometer on NIMBUS-7 to remove sudden discontinuities not present in the Mg II record. Degradation in early solar radiometers is difficult to quantify, as many did not have multiple channels for on-orbit tracking. To overcome this liability, Fröhlich fits a degradation correction to the early measurements by the Hickey-Frieden solar radiometer that is similar to the quartz siliconizing parameterization that he uses to account for analogous sensitivity changes detected in the more-recent Variability of Solar Irradiance and Gravity Oscillations (VIRGO)/Physicalish-Meteorologisches Overvatorium Savos (PMOD) radiometer. The new composite, similar to the prior ones, shows no significant secular change in irradiance, but does show a somewhat different behavior of cycle 21.

Secular changes in irradiance are an important area of on-going research. **Tom Woods** (LASP, University of Colorado) discussed possible changes

Figure 6: The solar irradiance spectrum is shown shortward of 2000 nm along with the estimated variability of the irradiance over the 11-year solar cycle. At the short ultraviolet wavelengths, the solar variability is larger than the solar minimum irradiance value, and the variability at the visible and infrared wavelengths is about 0.1% of the irradiance value. As listed in the table, the ultraviolet irradiance is a small amount of the total solar irradiance (TSI), but the ultraviolet variability is a more significant part of the TSI variability.



Range	Fraction of TSI	Fraction of TSI SC Variation
0-400 nm	7.7%	24%
0-300 nm	1.1%	12%
0-200 nm	0.008%	1.2%

in solar irradiance during the Maunder Minimum period of the late 1600s, when sunspots were absent from the Sun for long periods. Based primarily on analysis of solar Ca K images (which indicate regions of facular brightness), Woods pointed out that solar active regions alone, as indicated by sunspot numbers, cannot account for the expected lower irradiances that are obtained by removing known brightness sources present in the Ca K images even during solar-cycle minima. He suggests that an absence of the active network caused lower irradiances at this time. Estimated irradiance variations between the most recent 1996 solar minima and the Maunder Minimum are as follows: the Ly-alpha irradiance was lower by 25%; the UV (<400 nm) irradiance was lower

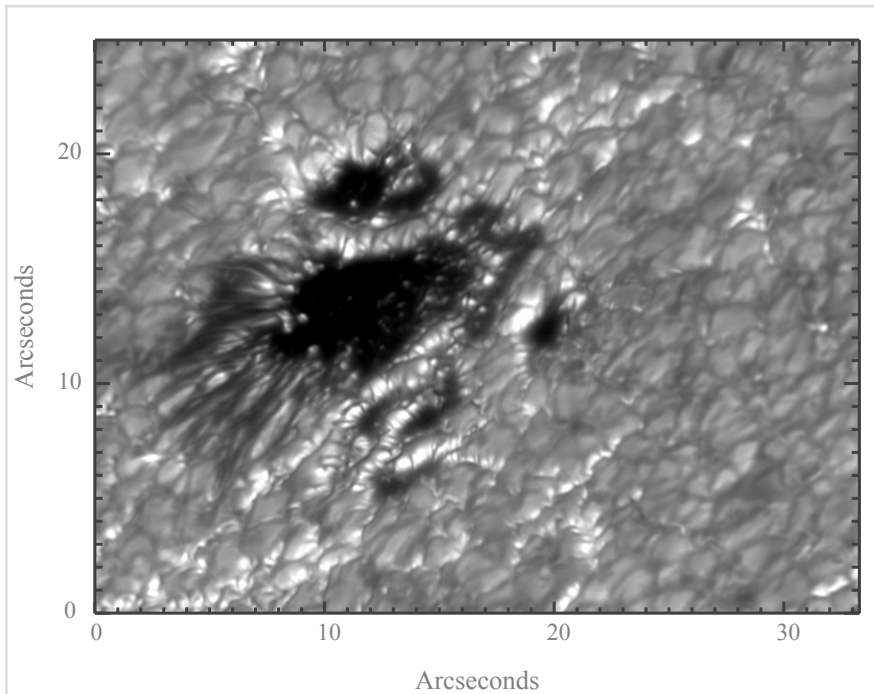
by 0.32 W/m², and TSI was lower by 1.3 W/m².

Continuing the topic of the role of faculae, **Ken Schatten** (ai-solutions, Inc., Lanham, MD) described his *Ion-Hurricane Model* for sunspots and faculae, and compared it to the conditions that create hurricanes on the Earth. He contrasted the fluid-dynamical solar-ion hurricane model to a quite different facular model—that of Spruit's field-inhibition hot-wall model. Two basic differences are that: 1) in the fluid-dynamical model the magnetic field enhances energy transport whereas in the field-inhibition model the field reduces it; and 2) faculae in the fluid-dynamical model appear as *hillocks* on the Sun's surface (uplifted structures with bright sides) rather than depressions or wells.

Thus, in the fluid-dynamical model, the Sun's magnetic field enhances the solar irradiance by allowing the Sun to shed its luminosity through a second energy transport mechanism, very much as a hurricane enhances energy transport from the oceans. This helps explain the overall effect of solar activity to enhance the Sun's luminosity. It is a challenging observational question to ascertain whether faculae are *uplifted* features, when there is no *sea level* on the Sun to measure the relative heights of features.

Wonderful new high-resolution images of the Sun's surface have been recently recorded, and may afford the possibility of clarifying mechanisms of faculae formation. **Tom Berger** (Lockheed Martin Solar and Astrophysics Laboratory, Palo Alto, CA) showed some of the best images and movies of faculae ever recorded. He compared images of solar faculae and magnetic field strengths with 0.1" resolution from the Swedish Solar Telescope. He described the observational challenges behind measuring facular area and center-to-limb variations. His high-resolution facular images will help validate whether the hot-wall field-inhibition model or that predicting *hillock* faculae is more realistic. 3-D compressible magneto-hydrodynamic simulations do well replicating the morphology of the observations, but currently lack the detail and the dynamic effects on short time scales seen in his movies. Mechanisms besides sunspots and faculae have been speculated to contribute to solar-irradiance variations on multi-decadal to millennial time scales. **Peter Foukal** (Heliophysics, Inc., Nahant, MA) showed that the evidence used over the past 10 years to argue for such additional variation is no longer valid. He also pointed out that satisfactory

Figure 7: Active Region 10377 taken on June 6, 2003 in the G-band 430.5 nm bandpass at a disk position of N5 E43 degrees heliographic. The image shows the three-dimensional form of bright faculae surrounding the central sunspot: faculae are the walls of granulation seen through the transparency caused by the small-scale magnetic field outside of sunspots. (Tom Berger)



physical explanation of the spot- and facular-induced irradiance fluctuations requires that the enormous thermal inertia of the Sun's convective envelope be taken into account. In Foukal's view, this inertia limits any additional irradiance variations associated with conceivable solar structural changes to relatively shallow layers. More-precise solar photometry will be required to search for such—as yet undetected—mechanisms. In this regard, Foukal described the recent balloon flight of the Solar Bolometric Imager which was used to obtain the first wide-band (0.2-3 μm) facular contrasts. These new contrasts should enable construction of more-accurate empirical irradiance models using the long time series of facular areas compiled at San Fernando Solar Observatory, a topic he is pursuing with Steve Walton of CSUN. In contrast with Tom Wood's earlier discussion (see **Figure 6**) he concluded

that, at present, evidence favors long-term solar output variations of amplitudes limited ($<0.1\%$) and comparable to those observed over recent decades.

Session 4—Climate Variability Modes, e.g., ENSO, NAO/AO, PDO, and Non-linear Response

Chairs: Lesley Gray (Reading University, UK) and Peter Pilewskie (LASP, University of Colorado)

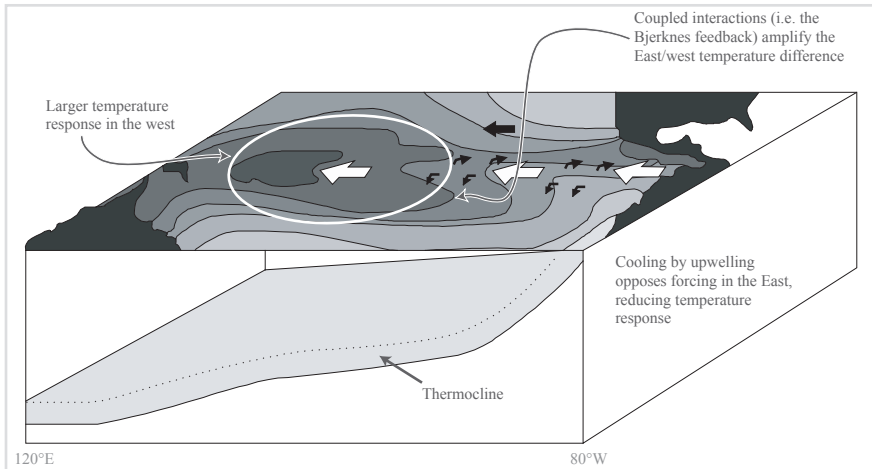
Session 4 began with **Mark Cane** (Lamont-Doherty Earth Observatory of Columbia University) providing an excellent overview of the basic mechanisms of the El Niño/Southern Oscillation (ENSO) and its impacts around the globe. He addressed the Bjerknes feedback, (see **Figure 8**) potentially a key amplifying mechanism in the climate's response to solar variability. ENSO influence goes well beyond the tropical Pacific, affecting

worldwide patterns. The response is mediated by the *thermostat mechanism* whereby a positive forcing leads to a colder eastern equatorial Pacific and an increased zonal temperature gradient on the equator. He concluded with a long-term perspective on ENSO that comes from paleoclimate records and models that show a response to natural solar and volcanic forcing.

Amy Clement (Rosenstiel School of Marine and Atmospheric Sciences, FL) explained her investigation into the response of El Niño to volcanic and solar forcing over the past 1000 years. She found that very small decadal sea-surface temperature (SST) anomalies can have large impacts on climate. A combination of responses to past changes in volcanic and solar radiative forcing closely reproduces changes in the mean state and interannual variability in El Niño in past centuries which have been recorded in fossil corals. She suggested that droughts in the American west are directly related to small anomalies in tropical Pacific sea SSTs and raised the question, "Can these anomalies be related to variability in solar irradiance?"

Evidence exists for decadal time-scale periodicities in the instrumental and proxy climate records that may be related to solar forcing, according to **Michael Mann** (University of Virginia, Charlottesville). A leading expert in the statistical description of climate variability, Mann reviewed work looking at both the statistical connections and underlying dynamical mechanisms for solar forcing of climate on decadal-through-multicentennial time scales. The decadal time-scale signals suggest both thermodynamic and dynamical responses of the climate to solar radiative forcing. Proxy-based climate reconstructions suggest persistent

Figure 8: This figure is a schematic of the mechanism by which a heating of the tropical Pacific ocean can lead to a cooling in the eastern equatorial Pacific. The heating produces a larger temperature response in the western basin than in the eastern basin. This is because the effect of upwelling of cold water into the surface offsets the forcing. As a result, there is a slight increase in the east-west temperature gradient that in turn accelerates the trade winds. The stronger trade winds lead to increased upwelling and a shallower thermocline, both of which cool in the east. This feedback between the surface temperature gradient, winds and thermocline is known as the Bjerknes feedback, which is the fundamental mechanism leading to El Niño events. As a result of this feedback, there is a cooling in response to a heating at the surface of the tropical Pacific ocean. (Amy Clement)



decadal and multidecadal relationships with solar forcing over centuries and millennia. Mann concluded that forced changes in large-scale atmospheric circulation such as the NAO, and internal dynamics related to El Niño, may play an important role in explaining regional patterns of response to solar forcing.

Atmospheric Centers of Action (COA) at the surface are extended regions of high and low pressures that dominate atmospheric circulations over large areas. It is useful to study the variations of the COA because they are strongly coupled to regional climate, as **Sultan Hameed** (Stony Brook University, NY) described in his talk at the 2003 SORCE meeting. This year, Hameed showed that two such COA, the Icelandic Low and the Azores High, are strongly related to regional climates in North America, Europe and North Africa while the Aleutian Low and the Hawaiian High are strongly related to regional climates in East Asia and

North America. The surface pressures and the positions of the Aleutian Low (see **Figure 9**), the Icelandic Low, the Hawaiian High, and the Azores High systems have significant correlations with the solar cycle when they are classified by the East and West phases of the QBO. The responses in the surface conditions of the COA are found to lag the stratospheric wind direction by zero to four months.

In an excellent complementary discussion to Mark Baldwin's keynote talk, **David Thompson** (Colorado State University, Fort Collins) addressed the impact of stratospheric ozone depletion on climate change at the Earth's surface. He suggested that recent southern hemisphere climate change can be interpreted as a bias towards the high-index polarity of the fluctuations in the strength of the circumpolar vortex pattern. The largest and most significant trends at Earth's surface can be traced to recent trends in the lower stratospheric polar vortex, which are largely

due to photochemical ozone losses. He concluded that stratospheric ozone depletion in the Southern Hemisphere is associated with substantial changes in climate at Earth's surface.

To explore mechanisms by which solar variability influences climate, **Alexander Ruzmaikin** (Jet Propulsion Laboratory [JPL], California Institute of Technology, Pasadena), investigated how the dynamics of the interaction between planetary waves and zonal flow responds to changes in solar UV flux. Using the assimilated data from the NCEP re-analysis, he showed that the extratropical signature of the QBO is seen mostly in the North Annular Mode (NAM). To understand these findings, Alexander researched earlier suggested mechanisms for extratropical manifestation of the QBO, and the time dependence of the QBO-NAM coupling.

Past and ongoing research (as John McCormack and Murry Salby described at the meeting) suggests that a solar-cycle influence in the lower atmosphere may be linked to the QBO, which is generated primarily by small-scale gravity waves. **Hans Mayr** (NASA Goddard Space Flight Center) recently initiated a 3D study where the QBO under the influence of the solar cycle was simulated. Preliminary results indicate that the Numerical Spectral Model (NSM) can produce a relatively large modulation of the QBO related to the solar cycle. Mayr discussed ideas about how the effect might be generated, but cautioned that further numerical experiments are needed to explore and more fully understand the mechanism that may amplify the solar-cycle influence. In addition, parametric studies with improved vertical and temporal resolution must be implemented to determine

whether the effect is real and the results are robust.

Zonal-mean ozone perturbations can affect the QBO. **Eugene Cordero** (San Jose State University, CA), examined this association during the 11-year solar cycle by using a model of the tropical stratosphere. The model accounts for wave-driven changes in the zonal-mean circulation and thus can simulate the zonal wind, temperature, and ozone QBOs in the tropical stratosphere. He concluded that solar-cycle-like perturbations to the ozone field affect the QBO in a way that resembles observations. Wave-induced ozone perturbations are apparently responsible for a majority of these changes. Future work is needed that will include upper stratospheric responses, the annual cycle, and eventually a global model.

Building on his recent seminal work on the role of the QBO in facilitating

solar forcing of the middle atmosphere, **Murry Salby** (Program in Atmospheric and Oceanic Sciences [PAOS], University of Colorado, Boulder) discussed the detection of a solar-cycle influence on the general circulation of the stratosphere, with subsequent interaction with the troposphere. Modulation of the QBO's phase during winter can explain the large amplitude of the solar signature when polar temperature is stratified against equatorial wind. Stratifying data rectifies the high-frequency oscillation, leaving a systematic drift through all phases of the solar cycle. The accompanying structure resembles interannual changes of the residual mean circulation of the stratosphere. The latter is characterized by anomalous downwelling over the winter pole, which penetrates well into the troposphere. Compensating it at subpolar latitudes is anomalous upwelling, accompanied by an apparent intensifi-

cation of the Hadley circulation. Similar structure characterizes changes that operate coherently with the QBO and solar activity.

Opening the Friday morning portion of this session, **Jose Rial** (University of North Carolina, Chapel Hill) began by discussing the (nonlinear) causes of abrupt climate change during the last Ice Age, and demonstrated with a simple model that variability in the Greenland Ice core Project (GRIP) short-period time series can be explained by non-linear oscillations externally forced by astronomically induced changes in incoming solar radiation. The model reproduced the Younger Dryas episode very well (see **Figure 10**) and thus may provide useful predictions of global warming at the millennial scale. The next challenge is to incorporate as many physical processes as possible by using the relevant climate variables, including geography, to demonstrate that the sea-ice/ocean/atmosphere thermal system is equivalent to a forced, self-sustained, nonlinear relaxation oscillator.

In his talk on the effect of ENSO on the dynamical and thermal structure of the middle atmosphere, **Fabrizio Sassi** (NCAR, Boulder, CO) presented a simulation using a General Circulation Model (GCM) forced with observed SST for the period 1950-2000. He showed that circulation anomalies in the middle atmosphere are accompanied by large temperature anomalies that are of opposite sign in the stratosphere and mesosphere. The findings were corroborated by an annular-mode analysis which showed that the strongest coupling between stratosphere and troposphere occurred during El Niño events when stratospheric sudden warmings were more frequent.

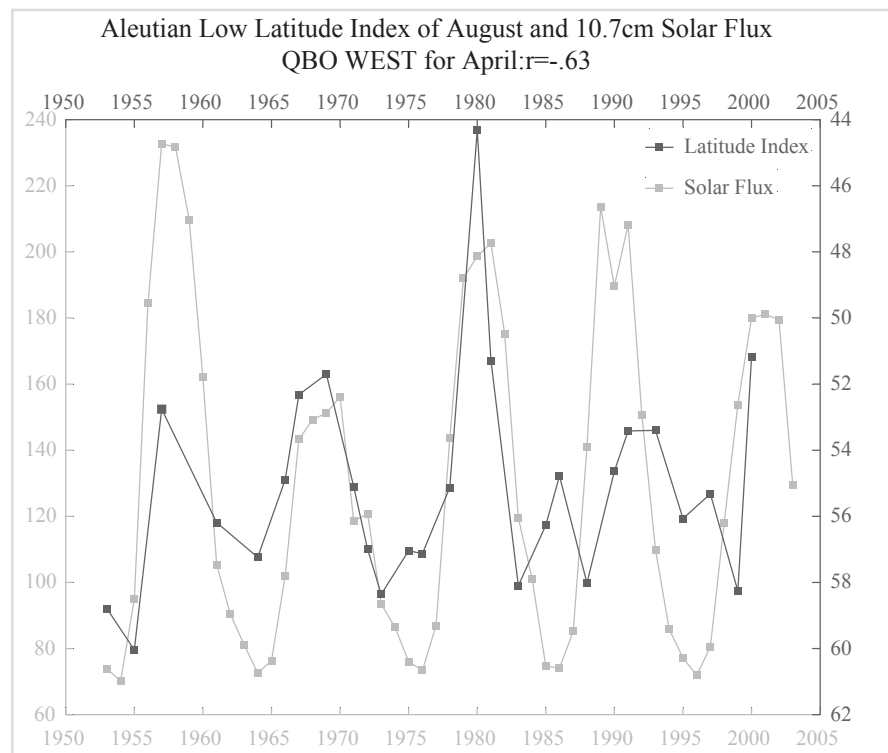
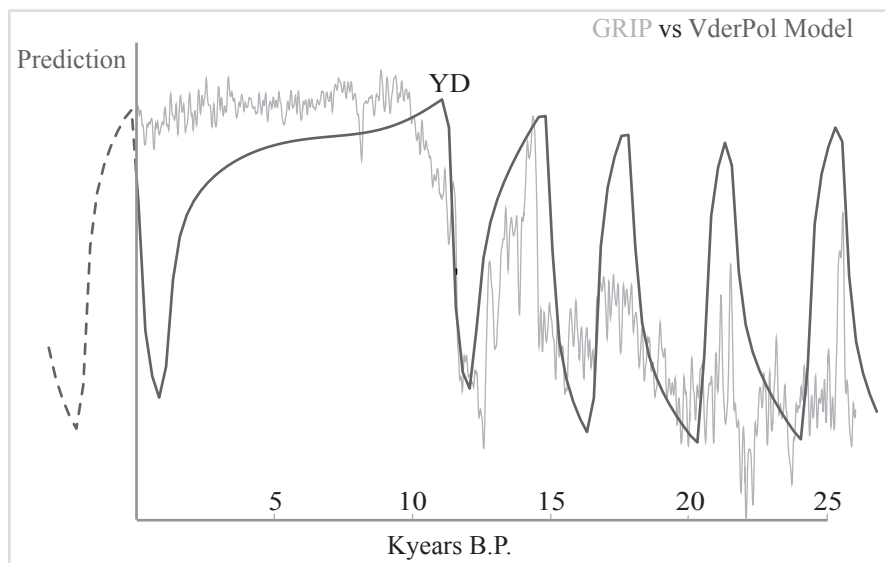


Figure 9: The correlation of the Aleutian Low latitude position in August with the 10.7 cm Solar Flux when the winds at 30 mb are westerly. Significant correlations exist for westerly wind directions in August, July, June, May and April, and the last case is shown in this figure. (Sultan Hameed)

Figure 10: Detail of the comparison between the van der Pol model and the GRIP time series. The model is the result of forcing a 2.75ky nonlinear thermal oscillator (sea ice-ocean-atmosphere) with the theoretical insolation. The period of the oscillator was extracted from the data by frequency demodulation. The model reproduces the phases and some of the amplitudes closely, and is robust to changes in the parameters. The “prediction” for the next 2,000 years is suggestive. Work is in progress to confirm the existence of the 2.75ky oscillation using a general circulation model. YD marks the Younger Dryas episode. (Jose Rial)



Using the moon to monitor terrestrial albedo was the theme of **Enric Pallé's** (Big Bear Solar Observatory, CA) paper on changes in the Earth's albedo over the past two decades. Observations from the illuminated and dark sides of the moon obtained at Big Bear Solar Observatory were correlated with satellite-measured global cloud cover to derive a proxy for solar reflectance. The results indicate a decrease in reflectance from 1984-2000. Since 2001 this trend appears to have reversed. New measurements of lunar-reflected earthshine are spectrally resolved and thus may reveal global trends in absorbing species such as ozone and water vapor.

Shuntai Zhou (NOAA/NCEP, Camp Springs, MD) examined a Sun-climate link through the response of stratospheric zonal wind and other dynamical factors to solar-cycle variations, determined using 24 years of observed data. While the zonal-wind sensitivity to solar-cycle variations was found to

be relatively small compared to other factors, it was significant in the tropical upper stratosphere and in the extratropics of the southern hemisphere.

The 2004 SORCE Science Meeting concluded with **Shaopeng Huang** (University of Michigan, Ann Arbor) reporting a fascinating concept to retrieve information about past solar irradiance from lunar regolith temperatures, as well as the radiation budget of Earth. Temperature time series at the Apollo 15 landing site revealed the diurnal cycle and trends in near-side lunar-surface temperature driven by direct solar irradiance during the day and reflected solar radiation and longwave emission from Earth at night. Huang suggests that subsurface temperature measurements from boreholes on the Moon can provide valuable extensions of the length of the lunar-surface temperature history, and of its relationship to radiative variations in both the Sun and the Earth.

Science Dinner

On Thursday evening **Dan Schrag** (Harvard University) entertained attendees following dinner at a ski lodge by talking about “*Snowball Earth and Other Climate Tales of Earth and Her Neighbors.*” Many lines of evidence support a theory that the entire Earth was ice-covered for long periods 600-700 million years ago. Each glacial period lasted for millions of years and ended abruptly under extreme greenhouse conditions. These climate shocks triggered the evolution of multicellular animal life and challenge long-held assumptions regarding the limits of global change. The geological record hosts multiple extraordinary observations that can all be explained by the *snowball Earth* hypothesis. The appeal of the hypothesis is that it simultaneously explains all of these salient features of the geologic record, none of which had satisfactory independent explanations.

Poster Sessions

Session 1. Solar Radiation—Status of Current SORCE Measurements

A Comparison of the VIRGO and TIM Data, by Claus Fröhlich, Physikalisches-Meteorologisches Observatorium Davos, Switzerland

The SOLSTICE Observing Technique, by Marty Snow, LASP, University of Colorado, Boulder

SORCE Science Data Processing and Availability, by Christopher Pankratz, LASP, University of Colorado, Boulder

Session 2. Decadal Variability in the Atmosphere and Oceans

Figure 11: Marty Snow from LASP discusses his poster on the role of spectral resolution in measuring the solar magnesium II index. There were 17 posters featured during the meeting, with a special poster reception on Wednesday afternoon.



Global Measurements of the Earth's Visible Spectral Albedo, by Pilar Montanes-Rodriguez, Big Bear Solar Observatory (New Jersey Institute of Technology), California

Vertical Propagating Wave Diagnostic Analysis, by Alfred M. Powell, NOAA/National Environmental Satellite, Data, and Information Service/Office of Research Applications (NESDIS/ORA), Camp Springs, Maryland

Relationships Between Solar Activity, Earth Rotation and Atmospheric Angular Momentum, by David Salstein, AER, Inc., Lexington, Massachusetts

A Solar-Cycle Influence on New England's Climate?, by Richard Wolfson, Middlebury College, Vermont

Response of the O(1S) Dayglow to the Solar Zenith Angle and Solar Irradiance: An Empirical Model by WINDII on UARS, by Shengpan P. Zhang, CRESS, York University, Toronto, Canada

Session 3. Mechanisms and Modes of Decadal Solar Variability

Measurement of the Long-Term Total Solar Irradiance Trend: What is Needed Versus What is Achieved, by Steven Dewitte, Royal Meteorological Institute of Belgium, Brussels

Some Thoughts about the Reliability of Reconstructions of Total Solar Irradiance into the Past, by Claus Fröhlich, Physikalisch-Meteorologisches Observatorium Davos, World Radiation Center, Davos Dorf, Switzerland

Inferring Total Solar Irradiance from Sunspot Areas Only, by Dora G. Préminger, San Fernando Observatory, California State University, Northridge

Direct and Indirect Thermospheric Heating Sources for Solar Cycles 21-23, by D. J. Knipp, U.S. Air Force Academy, Colorado Springs, Colorado

The SUSIM MgII Core-to-Wing Ratio Index, by Linton E. Floyd, Interferometrics, Inc. and Naval Research Laboratory, Washington, DC

The Role of Spectral Resolution in Measuring the Solar Magnesium II Index, by Marty Snow, LASP, University of Colorado, Boulder (see **Figure 11**)

Center-to-Limb Variation of the Solar UV Spectrum Observed by SKYLAB, by Jeff Morrill, Naval Research Laboratory, Washington, DC

Empirical Orthogonal Function Analysis of Solar Spectral Irradiance from SIM, by Guoyong Wen, NASA Goddard Earth Sciences and Technology Center (GEST)/University of Maryland Baltimore County (UMBC)

NOAA NESDIS Data Rescue Solar Image Scanning Project, by Helen E. Coffey, NOAA National Geophysical Data Center, Boulder, Colorado

Plans for the next *SORCE* Science Meeting are already underway. The next meeting will vastly extend the time domain to paleoclimate and the very-longest-term changes in the solar output. Everyone is welcome! Please mark your calendar for September 14-16, 2005 and stay tuned to the *SORCE* website: lasp.colorado.edu/sorce/meetings.html for details. We plan to meet in southwest Colorado.

Acknowledgements

The authors are pleased to acknowledge the following individuals for their contributions to the *SORCE* mission and this Science Team Meeting:

Vanessa George was responsible for all details of the meeting—both large

and small. She arranged the location and insured that weather cooperated beautifully.

SORCE Team Members: **Jerry Harder, Greg Kopp, George Lawrence, Bill McClintock, Tom Woods.** All are at LASP, University of Colorado, Boulder.

Session Chairs: **Robert Cahalan**, NASA Goddard Space Flight Center; **David Rind**, Goddard Institute for Space Studies, Columbia University; **Stephen Walton**, San Fernando Observatory, California State University, Northridge; **Lesley Gray**, Reading University, Reading, United Kingdom; **Peter Pilewskie**, LASP, University of Colorado, Boulder

Meeting speakers, presenters, and attendees whose shared enthusiasm and expertise contributed much to the meeting's success.

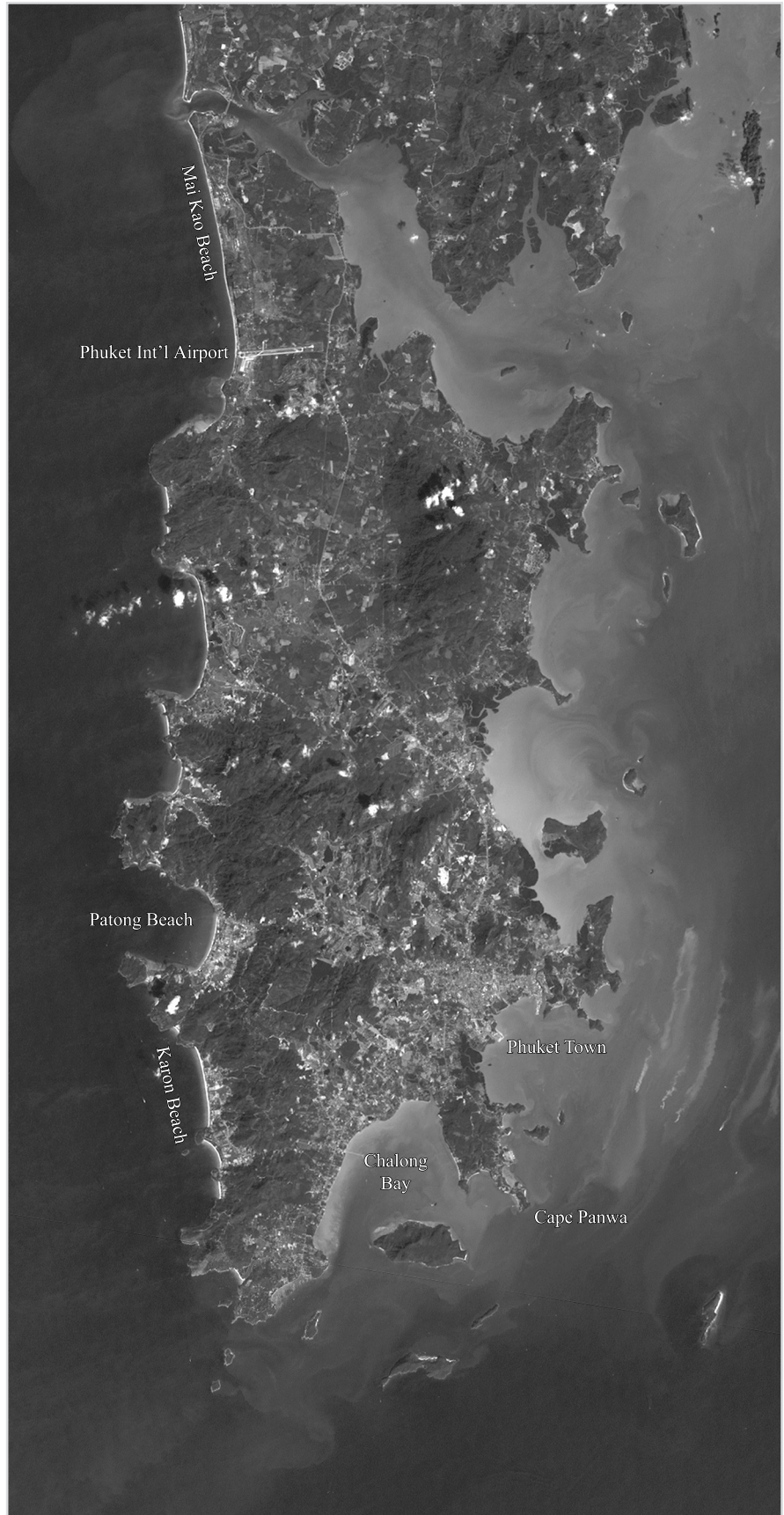
For additional information on the SORCE Mission, see the SORCE website at lasp.colorado.edu/sorce/ for the latest news and updates.



The island of Phuket on the Indian Ocean coast of Thailand is a major tourist destination, with inviting white sand beaches and warm sunny skies. Unfortunately for those living and visiting there to escape the Northern Hemisphere's winter gloom, it was also in the path of the Asian tsunami that washed ashore on December 26, 2004. This Landsat 7 Enhanced Thematic Mapper Plus (ETM+) satellite image shows how the island appeared on December 27, 2000, well before the wave of destruction.

It was the beaches that bore the brunt of the massive waves, which probably struck the west coast (left side) within an hour of the undersea earthquake. Devastation was particularly severe in Patong and Karon Beaches.

NASA image created by Jesse Allen, Earth Observatory, using data obtained from the University of Maryland's Global Land Cover Facility.



Minutes of the Aqua Science Working Group Meeting, October 26-27, 2004

— Claire L. Parkinson, *claire.l.parkinson@nasa.gov*, NASA Goddard Space Flight Center
 — Steven Platnick, *steven.platnick@nasa.gov*, NASA Goddard Space Flight Center
 — Steve Graham, *steven.m.graham.2@gsfc.nasa.gov*, NASA Goddard Space Flight Center
 — Moustafa T. Chahine, *moustafa.t.chahine@jpl.nasa.gov*, NASA Jet Propulsion Laboratory

The Aqua Science Working Group met at NASA Goddard Space Flight Center (GSFC) on October 26-27, 2004, with an Opening Session summarizing the status of many aspects of the Aqua mission, followed by two workshop sessions concentrating on cloud retrievals and water vapor validation, respectively.

Opening Session

Chair: Claire Parkinson, NASA GSFC

Introduction and Spacecraft Status

The meeting was opened by Aqua Project Scientist **Claire Parkinson**, who welcomed the group, went over a few adjustments to the agenda, thanked the attendees for coming, and provided the following updates:

- On October 20-21, 2004, the Afternoon Constellation (A-Train) Mission Operations Working Group met at GSFC. Aqua is now joined in the A-Train by Aura, which was launched on July 15 and is sending down science data from three of its four instruments. PARASOL (see end of article for a list of acronyms) is scheduled to be launched in December 2004, CloudSat and CALIPSO in May 2005, and the Orbiting Carbon Observatory (OCO) in 2008. The two science presentations at the A-Train meeting were by Parkinson and Ernest Hilsenrath, the Deputy Project Scientist for Aura. Afterwards, Hilsen-

rath kindly agreed to present again the status report he gave on Aura science, which included interesting comparisons with Aqua data, at the end of this Opening Session of the Aqua Science Working Group meeting.

- A Memorial Symposium in honor of Al Chang was held at the GSFC Visitors Center on October 12. Chang was the Deputy Project Scientist for Aqua for many years and was a member of the AMSR-E Science Team, developing the continental snow algorithm. He died in his office at GSFC on May 16, 2004. The memorial symposium was a full day honoring Chang's work in many arenas, including his contributions to the Canadian program in passive microwave sensing of snow and his contributions to remote sensing in Taiwan, in addition to his work at NASA. Among his accomplishments, Chang helped found several remote-sensing institutes in Taiwan.

- The October 2004 AMSR-E Antarctic Sea Ice (AASI) campaign succeeded in accomplishing one validation flight over the sea ice in the Weddell Sea and two flights over the sea ice in the Bellingshausen Sea, before officially ending on October 25 due to problems with the P-3 aircraft. The goal had been for six validation flights, and although that goal was not reached, a considerable amount of validation data was collected during the three successful flights.

- The front page of the September 2004 issue of the Joint Center for Satellite Data Assimilation (JCSDA) Quarterly has the prominent headline: "Science Update: AIRS Data Improve Global Forecast Accuracies."

- Several NASA Research Announcements (NRAs) relevant to Aqua scientists were released in 2004. Oceans and Ice NRA proposals were due May 4, and the review panels for them met in August and September. NASA Energy and Water Cycle Sponsored Research NRA (NEWS) Step 1 proposals were due August 24, and proposers were notified in late October as to whether they were or were not encouraged to submit full Step 2 proposals, due December 17. Over 400 Step 1 proposals were submitted, and the submitters for over 200 of them were encouraged to proceed. Proposals for Measurements, Modeling, and Analyses in Support of Aura and Other NASA Satellite Observations of the Earth's Atmosphere were due August 30, and 249 proposals were submitted, several from Aqua team members. Finally, NASA released an education NRA and an outreach NRA in 2004, with proposals due on September 28 and October 14, respectively.

Following Parkinson, the Aqua Mission Director **Bill Guit** summarized the state of the Aqua spacecraft, which is continuing to perform excellently, and generously offered to provide a

tour of the Mission Control facilities to any interested attendees. Guit had the encouraging news that, if the funding for mission operations continues to be available, Aqua could exceed its six-year designed lifetime by a factor of 2 or 3. He is looking forward to the remaining satellites in the planned Afternoon Constellation (the A-Train) being added to the currently flying Aqua and Aura missions. Recent work toward that end has included development of the Afternoon Constellation Operations Coordination Plan and the performance, over the past two months, of a series of inclination-adjust maneuvers by Aqua and Aura. These maneuvers have positioned Aqua and Aura appropriately so that they will need no additional maneuvers during the designed lifetimes of the next three members of the A-Train (PARASOL, CloudSat, and CALIPSO). This spares these smaller members of the Constellation from having to use fuel for any inclination-adjust maneuvers. As currently planned, the next set of inclination-adjust maneuvers for Aqua and Aura will be in the fall of 2007.

During the question period following Guit's talk, **Michael King** mentioned the large amount of space debris in the A-Train orbit, and Guit confirmed that there are 1500 pieces of catalogued debris, all of it man-made. This is about 15 times the amount of debris in the lower orbit of the Space Station. Despite the amount of debris, however, so far there has been no occasion when Aqua has had to perform a debris-avoidance maneuver.

NASA Headquarters Perspective

Jack Kaye, the Director of the Research & Analysis Program of the Earth-Sun System Division at NASA

Headquarters, provided an overview from the Headquarters perspective. He began with a statement that this is a wonderful time of Earth-science accomplishment at NASA, with many Earth-observing satellites in orbit, other satellites planned for future launches, and much science being done with the data in hand. Kaye mentioned several high-level programs in which NASA is heavily involved, including the Administration's Climate Change Research Initiative, and the fact that Earth observations are now important politically, both nationally and internationally. Furthermore, the vision for exploration unveiled by President Bush in January 2004 does not alter the fact that NASA's mission continues to include, prominently, the aim "to understand and protect our home planet".

A Commission chaired by Pete Aldridge was charged in February 2004 to determine how NASA could implement the exploration vision. This Commission issued a report in June 2004 that encouraged the transformation that NASA is currently undergoing. Kaye showed a chart of NASA's Transformed Structure, centered on four mission directorates: Exploration Systems, Space Operations, Science, and Aeronautics Research. The Science Mission Directorate is further divided to the Earth-Sun System, Solar System, and Universe divisions. The Earth-Sun System Division has three subgroups, one of which is the Research & Analysis Program headed by Kaye. Jim Garvin was recently named NASA Chief Scientist.

On request from NASA, the National Research Council is beginning a decadal study on Earth Science and Applications from Space, encompassing both NASA and NOAA satellite observations and

cochaired by Berrien Moore and Rick Anthes. The first major meeting for this effort was held in August 2004 in Woods Hole, and the second is planned for November 9 in Washington, D.C. Kaye commented that determining the appropriate role of NASA in space sciences is more straightforward than determining the appropriate role of NASA in Earth sciences, where other agencies are also involved.

Kaye anticipates an annual integrated NASA Earth and Space Science research announcement presenting the full scope of funding opportunities planned for the year. This expands, to include Earth sciences, a policy already successfully implemented for NASA's space science program.

Referring back to Guit's comment that Aqua has the capability of remaining in orbit well beyond its designed life, Kaye mentioned that as functioning satellites pass their designed lifetimes, NASA examines on an individual basis whether to provide the additional funds for continued mission operations. Currently the Tropical Rainfall Measuring Mission (TRMM) is being kept operational at least through the 2004 hurricane season because of its practical importance for hurricane monitoring. Keeping it operational, of course, benefits the science as well, by lengthening the TRMM record.

The President's FY2005 budget is, at the time of this meeting, under consideration on Capitol Hill. The Senate has not recommended major cuts from the NASA Earth-science budget, but the House has recommended two targeted cuts, from the Orbiting Carbon Observatory and the Glory satellite mission. Kaye commented that it remains uncertain what will happen when the House and Senate go into conference.

On another budget issue, Kaye confirmed that NASA continues to struggle with the transition to full-cost accounting. However, he mentioned that since NASA's Jet Propulsion Laboratory (JPL) has worked in a full-cost environment for several decades, the NASA civil-servant centers presumably will be able to make an appropriate adjustment to full-cost accounting as well.

In closing, Kaye mentioned that NASA will soon be posting job announcements for three program manager positions in his group. Kaye has enjoyed his career at NASA Headquarters and recommends that others consider the opportunities now opening. He suggested that any attendees potentially interested in these positions please come and talk with him about them.

U.S. AMSR-E Science Team

Dawn Conway of the University of Alabama gave the U.S. AMSR-E Science Team progress report, substituting for the U.S. AMSR-E Science Team Leader Roy Spencer, also of the University of Alabama. Spencer was unable to attend because of a sudden severe illness in his family.

Conway began by mentioning the successful AMSR-E science-team meeting held in Fort Collins, Colorado in August, the minutes of which were published in the previous issue of *The Earth Observer* (vol. 16, no. 5, pp. 7-14, September/October 2004). In conjunction with the science team meeting, there was a workshop held the previous day regarding the Wakasa Bay precipitation measurements collected during a validation campaign in early 2003. Also in August 2004, AMSR-E scientists participated in a Soil Moisture Experiment (SMEX04) in Arizona.

A SMEX04 workshop is planned for May 2005. Conway also mentioned that in September 2004 there was an AMSR session at the IEEE Geoscience and Remote Sensing Society annual meeting (IGARSS04) in Anchorage, and that a joint Japan/U.S. AMSR-E Science Team meeting is scheduled for early December in Japan. She confirmed Parkinson's earlier comments regarding the partial success of the just-completed AASI validation campaign.

Conway explained that the first reprocessing of AMSR-E data is now complete. A new calibration from the Japan Aerospace Exploration Agency (JAXA) is scheduled to be implemented by February 2005. The next reprocessing of the AMSR-E data will then begin in May 2005, using the revised calibration from JAXA, the latest calibration from Remote Sensing Systems (RSS), and the latest AMSR-E Science Team algorithms.

Conway concluded by mentioning that validation of the AMSR-E algorithms continues, with some algorithms expected to be validated by May 2005. In particular, the Level 2A data are anticipated to be validated prior to the next reprocessing of the AMSR-E data.

Japanese AMSR-E Science Team

The Japanese AMSR-E Science Team Leader, **Akira Shibata** of the Japan Aerospace Exploration Agency (JAXA), presented a summary for the Japanese team. The AMSR-E instrument is operating well except for the 89 GHz A-horn vertical-polarization receiver, whose output is degrading. Shibata explained that the degradation started just after the Aqua launch and showed a plot of the receiver output for 2004, including projections through the end

of the year. The rate of degradation has varied between approximately -0.25 mV/month and 0 mV/month, with the current rate of degradation being -0.05 mV/month.

Shibata mentioned that all 15 Principal Investigator algorithms have been tested and are now being run at the Earth Observation Research Center (EORC). He listed the eight standard algorithm products that are currently being produced operationally: water vapor, cloud water, precipitation, sea-surface wind speed, sea-surface temperature, sea ice, snow, and soil moisture.

The Japanese AMSR-E Team conducted three field experiments in 2004: a soil-moisture experiment in Mongolia (to be continued through and beyond 2005), a snow-depth experiment in Siberia (ongoing until March 2005), and the AASI sea-ice experiment in the Antarctic, the latter done in cooperation with the U.S. AMSR-E Team. Furthermore, the Japanese Team continues to analyze field data from the 2003 Wakasa Bay experiment, 2003 Miyako-Yaeyama rain-gauge observations, and upward-looking microwave observations of water vapor and cloud liquid water from two islands.

Shibata explained that version 2 of the Level 1 AMSR-E data will be released in February 2005. These data will have corrections for 6-GHz non-linearity, for 6-GHz scan bias, and for geolocation errors.

The Japanese are also using the AMSR-E data in several practical applications. Specifically, the Japan Meteorological Agency (JMA) intends to begin using the AMSR-E data by the end of 2004 for short-range weather forecasting in the vicinity of Japan, and JMA and the

Japan Fisheries Information Service Center are both using the AMSR-E sea-surface temperatures (SSTs) on a routine basis.

CERES Science Team

The CERES Science Team Leader, **Bruce Wielicki** of NASA Langley Research Center (LaRC), presented the CERES summary, beginning with a list of new science efforts being undertaken by the CERES Team. Some of the key items on this list were:

- CERES is a major participant in the GEWEX International Radiative Flux Assessment program, which is now underway and is cochaired by Wielicki and three others.
- The 1992-2002 global net radiative fluxes from the Earth Radiation Budget Satellite (ERBS) and CERES have been found to agree with those from the Global Ocean Heat Storage program to within 0.3 W/m^2 .
- The CERES Team is working with a space-science group that recently reported increases in Earthshine (sunlight reflected from the Earth to the moon and then back to the Earth) over the period 2000-2003, countering the decreases found with the CERES data. The contrasting results are being compared and analyzed.
- A new analysis has been done comparing the CERES cloud properties and radiative fluxes with cloud-resolving models and the European Centre for Medium-range Weather Forecasts (EC-MWF) global model. Results have been submitted for publication.
- Several new studies are being initiated or proposed, including a

combined CERES/AIRS isolation of the far-infrared wavelength region, a combined CERES/AMSR-E analysis of cloud liquid-water path and multi-layer cloud properties, a new collaboration with climate modeling groups to examine satellite cloud and radiation data in a multi-model framework, and an eventual merged CERES/CloudSat/CALIPSO product once the CloudSat and CALIPSO members of the A-Train have launched and are operational.

Wielicki explained that Aqua Level 1 and ERBE-like top-of-the-atmosphere (TOA) fluxes are available. Aqua Level 2 TOA, surface, and atmospheric fluxes and angular distribution models (ADMs) are in production, but are given lower priority in the production process than the Terra CERES products. Still, the expectation is that a full three years of Aqua Level 2 products will be archived by summer 2006. Once the ADMs are complete, the Aqua Level 3 products will be produced, lagging the Level 2 products by about one month. Also, the CERES Team will be adding daily-average products to the 3-hourly and monthly products already being produced.

Wielicki showed a plot illustrating the need for $0.3 \text{ W/m}^2/\text{decade}$ accuracy in radiative flux measurements for quantitatively tackling the issue of global cloud feedback. The combined ERBS/CERES data set is the first to reach this 0.3 W/m^2 accuracy level. Wielicki then presented overlaid time series of ocean heat storage and ERBS/CERES global net radiation anomalies, showing how closely the two track each other. Responding to a question from the audience, Wielicki explained that, despite the lag in some ocean variables, anomalies in the total ocean heat storage should indeed be in phase

with anomalies in the net radiation, as the plot shows.

The CERES Science Team has been asked to assist in the planning for the National Polar-orbiting Operational Environmental Satellite System (NPOESS). As part of that process, they have determined the probability of having a gap in the radiation-budget measurements under various scenarios, and Wielicki included a very informative plot presenting those results. Assuming that the Terra and Aqua missions are funded to continue operations as long as they are able to, there is a 25% risk of a gap in the radiation-budget measurements from the CERES on Terra and Aqua by the year 2018. However, if the CERES flight model 5 (FM-5) is placed on NPOESS, the risk of a gap in the radiation measurements from CERES on Terra, Aqua, and NPOESS by 2018 is down to about 17%; and if FM-5 is placed on the NPOESS Preparatory Project (NPP) and the Earth Radiation Budget (ERB) instrument is placed on NPOESS, then the risk of a radiation-budget gap by 2018 is down to only 5%.

AIRS/AMSU/HSB Science Team

The AIRS Project Scientist, **George Aumann** of the Jet Propulsion Laboratory (JPL), presented the AIRS/AMSU/HSB summary, beginning with a listing of the Level 1B and Level 2 standard products, their RMS accuracy requirements, and the current estimates of their RMS accuracy. The Level 2 temperature profile, humidity profile, total precipitable water, and cloud-cleared infrared radiances, with current accuracy estimates of 1 K, 15%, 5%, and under 1.0 K, respectively, have all met their requirements for non-frozen ocean conditions. The sea-surface

temperature product, however, has not yet met the 0.5-K requirement, being at 1.0 K instead.

AIRS and AMSU (AMSU-A) continue in excellent health. Only 20 of AIRS's 2382 channels have experienced increased noise since launch, and 14 of those have recovered after temperature cycling. AIRS infrared radiometry is extremely stable, better than 8 mK/year, with absolute radiometry better than 0.2 K; and the AIRS spectral calibration is more accurate and stable than the ± 8 parts per million of the spectral response function centroid (ppmf) required for weather applications. Two channels of AMSU-A have experienced degradations in gain, but those have not affected the data products. AMSU stability is verified relative to equivalent AIRS channels under cloud-free conditions. (HSB provided high-quality data until February 2003 but has not worked since then.)

Aumann then summarized the use of AIRS data in data-assimilation efforts. Since May 2004, AIRS data have been used in the operational forecasts of the ECMWF and the U.K. Met Office. In the U.S., experimental assimilation is being done at NOAA's National Centers for Environmental Prediction (NCEP) and at the GSFC Laboratory for Atmospheres and the GSFC Global Modeling and Assimilation Office (GMAO). Aumann showed a plot from a paper by J. LeMarshall and others from the NOAA/NASA/Navy/Air Force Joint Center for Satellite Data Assimilation (JCSDA) illustrating the improvement in Northern Hemisphere 500-mb weather forecasts resulting from assimilation of AIRS data. The improvement in forecast skill at 6 days is considered equivalent to extending forecast capability by several hours.

Still, fewer than 1% of the AIRS data are being assimilated, and greater forecast improvements can be anticipated as more AIRS data are incorporated.

Atmospheric temperature profiles from the AIRS/AMSU data over non-polar oceans are considered accurate to 1 K per 1-km layer up to the 30-mb level of the atmosphere. Aumann estimates that AIRS is producing approximately 100,000 radiosonde-quality profiles each day. Regarding surface and near-surface measurements, Aumann showed a global surface air temperature map averaged for July 2003 and explained that this variable is more difficult to obtain than surface skin temperature, which is also obtained.

Comparisons with AMSR-E data show very good matches between AIRS/AMSU and AMSR-E total-water amounts under both clear and cloudy conditions. Aumann showed a map of upper tropospheric water vapor (above 600 mb) from AIRS/AMSU for July 2003. Measuring upper tropospheric water is very important for climate feedback. On average, the amount of water vapor above 600 mb is about 10% of the total atmospheric water vapor.

Aumann then turned from the standard AIRS/AMSU products to the research products and comparisons being generated by the AIRS Team. Research products and comparisons include carbon monoxide, ozone, sulfur dioxide, and aerosols, correlations between atmospheric Kelvin waves and humidity, and climate trends. The AIRS ozone product, obtainable under day and night conditions, compares well with the daytime ozone product produced from the Total Ozone Mapping Spectrometer (TOMS), which uti-

lizes ultraviolet radiation and requires daylight. Similarly, AIRS is yielding impressive aerosol results, as Aumann illustrated by showing a side-by-side comparison showing AIRS infrared and MODIS visible images of a dust storm over the eastern Mediterranean. The visible image vividly shows the dust storm, and the color-coded infrared image clearly corresponds well with the visible image, providing validation for the AIRS-derived product.

Aumann mentioned several plans for future work by the AIRS Team, including validation of Level 2 products over land and in high latitudes, version 4.0 reprocessing of the data, generation of global-emissivity maps to facilitate data assimilation over land, generation of global CO₂ and methane (CH₄) maps, and, later, determination of 5-year trends in mid-tropospheric temperatures. The team members also very much want to increase AIRS data utilization, both by the weather-forecasting community and by the science community. To facilitate that, they plan enhanced data subsetting for easier data access.

In summary, Aumann concluded by indicating that the AIRS Team is "raising the bar" regarding what can be accomplished with hyperspectral sounders.

MODIS Science Team

The MODIS Atmosphere Group Leader (and EOS Senior Project Scientist), **Michael King** of NASA GSFC, presented the MODIS summary, substituting for MODIS Science Team Leader Vince Salomonson, who was unable to attend. King showed a variety of products from the Terra and Aqua MODIS instruments, concentrating on the atmosphere.

The MODIS cloud mask, developed by Steve Ackerman and others at the University of Wisconsin, is generated at 250-m and 1-km resolutions and classifies pixels as “confident clear,” “probably clear,” “probably cloudy,” and “cloudy.” This product is used as input to many of the MODIS atmosphere and land algorithms, as well as algorithms for the MOPITT instrument on Terra. King showed a sample cloud mask image, followed by sample Terra MODIS images of cloud-top pressure and cloud optical thickness and effective radius. The images for the latter two variables distinguish ice clouds from water clouds through effective use of paired color bars.

The MODIS aerosol product was illustrated with images over the eastern U.S./western Atlantic and China. King explained that aerosol optical thickness is currently not obtained over bright land surfaces, such as deserts, snow, and ice, but will be eventually, aided by the development of a “deep blue algorithm” utilizing solar reflectance at wavelengths of 412, 490, and 670 nm, as described by Hsu *et al.* (2004, *IEEE TGARS*).

The MODIS precipitable water product was illustrated with images from both Terra and Aqua over the United States. Precipitable water is calculated from both near infrared and thermal infrared channels, with somewhat different results. (The basic patterns are the same from the two methods, but, in the example shown, the values were higher overall with the near infrared calculations.) King explained that for dry atmospheres the MODIS thermal-infrared calculation overestimates the total precipitable water but for most atmospheres it underestimates the precipitable water.

Global maps of April 2003 mean monthly cloud-fraction amounts from Aqua and Terra show very little overall contrast in cloud amounts between late morning (Terra) and early afternoon (Aqua). Quantitatively, in time series of global cloud fraction from July 2002 through July 2004, the afternoon measurements from Aqua average about 0.67 and the morning measurements from Terra average about 0.65. Both averages are well above the 50% cloud coverage that is frequently mentioned as a rough estimate of the overall global average. Like results from Aqua and Terra, those from the GLAS instrument on ICESat also indicate global cloud-cover averages of about 70%.

King then showed overlaid Aqua and Terra plots of zonal mean cloud optical thickness and zonal mean cloud effective radius, both for April 2004. For both variables, Aqua data tended, overall, to yield higher values over land than Terra data did but lower values over oceans.

King referred the listeners to the MODIS atmosphere web site, at modis-atmos.gsfc.nasa.gov, where many additional MODIS atmosphere data products and visualizations are available. He then explained and illustrated a joint effort between the MODIS atmosphere and land groups, producing a surface albedo product globally every 16 days.

MODIS Collection 4 reprocessing is now complete for both Terra and Aqua, with data processing proceeding forward for both MODIS instruments in near real time (typically only 1-2 days behind real time). Collection 5 enhancements and reprocessing are expected to begin about February 1, 2005 for the atmosphere products and about July 1, 2005 for the land products.

Aura, the Second Member of the Afternoon Constellation

The Deputy Project Scientist for Aura, **Ernest Hilsenrath** of NASA GSFC, provided an overview of the progress so far of the Aura mission, launched July 15, 2004, into an orbit lined up behind Aqua. Aura carries four instruments, all centered on atmospheric chemistry, and is the second member of the Afternoon Constellation (the A-Train) to be launched. The three central science objectives for Aura are: tracking the ozone layer, global measurements of air quality, and connecting atmospheric chemistry with climate.

Three of the four Aura instruments are working well, and Hilsenrath showed sample results from each of them. These three instruments are the Microwave Limb Sounder (MLS), the Ozone Monitoring Instrument (OMI), and the Tropospheric Emission Spectrometer (TES). The fourth instrument, the High Resolution Dynamics Limb Sounder (HIRDLS), appears to have something blocking its scan mirror, and efforts are underway to move the obstruction.

Early results from MLS include the first measurement of the hydroxyl radical (OH) in the middle atmosphere, multiple constituent (NO₂, HNO₃, H₂O, HCl, ClO, and O₃) and temperature measurements in the Antarctic ozone hole, and the global distribution of upper tropospheric water vapor. These measurements are obtainable even in the presence of water clouds. The OH measurements are particularly noteworthy; they are of better quality than anticipated and even show diurnal variations.

For early results from OMI, Hilsenrath showed global maps of total ozone,

south-polar animations of ozone and NO_2 , an NO_2 map of South America revealing areas of biomass burning, and a global map of aerosols. The OMI total-ozone results compare well with the ozone results from the highly regarded TOMS instrument. Furthermore, the OMI aerosol results provide a sharper image of local fires than the coarser-resolution TOMS, although, with a spatial resolution of about 13 km, the OMI results do not provide the spatial detail possible with MODIS (spatial resolutions of 250 m, 500 m, and 1 km).

TES results shown by Hilsenrath were four uncalibrated limb spectra, mapped tropospheric-ozone column measurements, and selected tropospheric-ozone profiles over the Atlantic. The TES spectral resolution is about twice as good as AIRS, and the TES tropospheric-ozone derivations can resolve several atmospheric layers between 1000 mb and 100 mb.

The Aura validation program includes nine planned major aircraft campaigns in the next three years and frequent mini-aircraft missions and ground-based measurements.

Hilsenrath concluded by mentioning science linkages between Aura and other members of the A-Train, including complementary measurements by OMI and AIRS of column ozone, by TES and AIRS of carbon monoxide, by OMI and MODIS of smoke and dust, by MLS, AIRS, and CloudSat of water vapor and clouds, by OMI and MODIS of cloud heights, and by HIRDLS, AIRS, and CALIPSO of cirrus clouds. With Aqua and Aura now both on orbit, inter-satellite comparisons among data products from A-Train instruments has begun.

Session 2a: Aqua Cloud Retrievals: Water Path

Chair: Steve Platnick, NASA GSFC

The second session, on cloud retrievals, was chaired by Deputy Aqua Project Scientist **Steve Platnick** and was divided into two sessions, a Tuesday afternoon session on cloud water path retrievals from AMSR-E, AMSU/HSB, and MODIS, and a Wednesday morning session on cloud-top properties from AIRS and MODIS, and cloud-data assimilation.

The AMSR-E, AMSU, and HSB microwave sensors retrieve liquid water path over the ocean, while the MODIS solar-reflectance technique estimates both liquid and ice water path and is applied over ocean and land surfaces. The cloud water path session was intended to foster an appreciation for the two techniques among the Aqua instrument teams and provide an impetus for collaborative work. Five speakers, representing each of these instrument teams, participated in the session. The talks provided an overview of the algorithms, discussed the strengths and weaknesses of the techniques, and presented example results and validation efforts. All participants agreed that comparisons between the microwave and MODIS retrievals are needed.

Microwave Liquid Water Path (LWP) Retrievals from AMSR-E

The first two water path talks discussed the microwave retrievals. **Frank Wentz** from Remote Sensing Systems (RSS) began with a general overview of the liquid water path algorithm that is common to the SSM/I, TMI, and AMSR-E sensors. A simplified form of the microwave radiative transfer equation was presented, emphasizing the

functional dependence of top-of-the-atmosphere (TOA) observed brightness temperatures on surface emissivity and atmospheric transmittance. Depending on frequency, transmittance is dominated by molecular oxygen, water vapor, and/or cloud water absorption. The ocean surface emissivity depends on wind speed as well as polarization. In addition, the condensed water index of refraction (cloud and ocean water) is a function of temperature. All AMSR-E frequencies/channels are used in the simultaneous retrieval of these quantities, which are then reported in the Ocean Products data files (Levels 2 and 3). The liquid water path retrieval is not sensitive to snow/ice particles. The retrieval assumes the water droplets are in the Rayleigh scattering regime, with drops small compared to microwave wavelengths. This approximation breaks down for precipitation, and therefore the retrievals assume that the cloud is not precipitating. The retrieval is linear with cloud fraction within the sensor field-of-view, as long as the water absorption is not too large, which is usually the case with non-precipitating clouds. The AMSR-E liquid water path retrieval has an expected accuracy (RMS) of 0.02 mm, with an upper limit of about ~0.2 mm that tends to correspond to precipitating systems.

Wentz then discussed the statistical modeling of retrieval error. This involves the analysis of the temporally and globally aggregated probability distribution functions (PDFs) of the ocean products. In particular, the occurrence of negative water path is not unexpected, due to measurement noise. A technique is used whereby zero water path, which is expected from analytic studies to correspond to half the value of the PDF mode, is used to scale the retrieval; misalignment can be due to

calibration or model error. Further, PDFs aggregated according to clear-sky screening from imager data can be used to indicate offset biases. This approach was used with TMI/VIRS data, and the clear-sky water path biases were found to be 0.008 mm. Wentz then showed scatter plots of AMSR-E water path vs. TMI and SSM/I (three instruments) for a one-hour observation coincidence window. There was good agreement with all instruments. Wentz concluded by stating that it is desirable to conduct similar comparisons with MODIS and AMSU/HSB retrievals.

AIRS/AMSU/HSB Total Liquid Water and Profile Retrievals

Phil Rosenkranz from the Massachusetts Institute of Technology (MIT) discussed the combined AMSU/HSB algorithm, which includes information about the water content profile in addition to the water path. The water path product is a standard product, while profiles are support (or research) products. The water content profile retrievals are used in AIRS processing to account for microwave absorption by clouds in the forward algorithm. Rosenkranz also discussed the impact from the loss of HSB data in February 2003 and summarized validation efforts.

Rosenkranz began with an overview of the algorithm. The algorithm uses AMSU window channels and HSB sounding channels to retrieve humidity profiles. Cloud water profile information essentially comes from the transmittance profiles and the assumption that layer humidity in excess of saturation indicates liquid water content. The algorithm first combines the higher spatial resolution HSB field-of-view within an AMSU footprint, then iterates

on temperature, water vapor, and liquid water profiles, as well as surface emissivity. An example of the importance of cloud profile information was demonstrated by showing the extent to which brightness temperature in the 52.8 GHz sounding channel depends on cloud altitude. Unlike other microwave algorithms, the AMSU/HSB algorithm provides retrievals over land, by taking advantage of the greater vapor absorption in HSB channels, reducing the impact of the variable land surface emissivity. The loss of HSB eliminates the capability for profile retrievals though there is some information on liquid water path over oceans from the AMSU water vapor and window channels. Over land or sea ice, both liquid-profile and liquid-path are now tagged with an "unusable" flag in version 4.0 when HSB is missing. As partial compensation for HSB, future efforts will attempt to integrate the AIRS IR water profile into the cloud retrieval.

Rosenkranz showed a one-day comparison between water path retrievals from AMSU/HSB and AMSR-E. Excluding precipitation scenes (as flagged by AMSR-E), the RMS difference was 0.050 mm. For precipitating scenes, AMSU/HSB retrievals overestimate the larger water paths (> 0.20 mm) relative to AMSR-E and underestimate the lower value water paths. Discussion at the meeting, however, revealed that the definition of the AMSR-E liquid-water path does not include the precipitating component, whereas the AMSU/HSB retrieval does. Comparisons with Atmospheric Radiation Measurement (ARM) Tropical Western Pacific (TWP; ocean) and Southern Great Plains (SGP; land) ground-based radiometric retrievals were shown next, with RMS differences of 0.05 and 0.126 mm, respectively. Also, the mean pressure of the retrieved liquid-water profile was compared

with the ARM radiosonde observation (RAOB) data (using relative humidity > 99% as a cloud indicator) for the HSB operational period (July 2002 - January 2003). Some skill was demonstrated for the TWP site (correlation of 0.43).

Liquid and Ice Water Path Estimates from Solar Reflectance Techniques: Examples from MODIS

Steve Platnick from NASA GSFC gave an overview of the MODIS liquid and ice water path retrievals that are produced as part of the operational MODIS Terra and Aqua cloud products (MOD06 and MDY06, respectively) archived at the Goddard Earth Sciences DAAC.

The relevant cloud retrievals from the solar-reflectance technique are optical thickness (τ) and effective particle radius (r_e). These are fundamental retrievals, whereas water path (liquid or ice) is a derived quantity that is proportional to the product of τ and r_e . Platnick derived the water path relationship for water and ice, noting that while water path and τ are vertically-integrated quantities, effective radius is, by definition, a local quantity that can and does vary with vertical position in the cloud. Therefore, the key assumption in estimating water path is that the cloud is homogeneous (droplet concentration and r_e constant with height). With regard to particle size, this either implies that r_e is constant throughout the cloud or that the retrieved r_e tends to give a weighting of the particle size profile that is consistent with the water path estimate; neither assumption is generally true. Platnick showed example water path biases calculated for vertically inhomogeneous water clouds and showed their dependence on retrieval spectral

band and cloud thickness. For the 2.1- μm band used in MOD06 retrievals, biases were typically less than 10%. Other issues related to solar-reflectance water path estimates include all items related to τ , r_e retrieval quality (cloud model assumptions, cloud detection, multilayer/multiphase cloud scenes, surface effects, etc.).

In comparison to microwave retrievals, the solar technique provides high-resolution retrievals (1 km for MOD06), though retrievals are, of course, only made for the daytime observations. On the other hand, thin ice clouds overlying water clouds can affect the water cloud retrieval, and thick ice clouds will completely mask the lower liquid cloud signal, so that the MODIS algorithm will report an ice water path. Such biases relative to the microwave retrieval need to be considered in comparing the two techniques. Further, the microwave retrieval effectively averages water path over the field-of-view, while MODIS assumes each 1-km pixel is either overcast or clear.

Platnick then discussed a pixel-level water path uncertainty estimate that will be produced in the next MODIS processing stream (collection 5); uncertainty is sensitive to τ , r_e , surface spectral albedo, and geometry. He then showed sample monthly Level 3 (gridded) data that were qualitatively compared with AMSR-E results. This was followed by an overview of MODIS liquid water path validation efforts, which have included TMI comparisons (R. Wood *et al.*, *GRL*, 2002), ship-board radiometer observations, and ARM SGP validation of ice-water path (Mace *et al.*, *JAM*, in press). Comparisons have been very encouraging, with agreement typically within the expected uncertainty range.

Evaluation of LWP from VIRS and MODIS for CERES

Pat Minnis from NASA LaRC gave an overview of MODIS water path retrievals that are being done in support of CERES data products. The overview included validations at the ARM SGP site and comparisons of LWP from the TMI radiometer on TRMM with LWP derived from the TRMM VIRS imager using the CERES algorithm. Like the MODIS operational cloud product described above, water path is derived from a product of the cloud optical thickness and effective radius retrieval; differences in the retrieval approaches include the CERES group's use of the 3.7- μm MODIS band for particle size information.

Minnis began by showing monthly global images of retrieved τ , r_e , and LWP for Terra and Aqua. Though the spatial patterns are similar, he noted that effective radii derived from Terra are less than those derived from Aqua, stating that the differences are thought to be primarily from a 3.7- μm calibration offset between the instruments, though perhaps partially reflecting a diurnal dependence as well. Global optical thickness and LWP were larger for Terra.

Minnis also presented a comparison between ARM SGP retrievals and MODIS retrievals. The SGP microwave LWP retrievals use the most recent ARM operational algorithm. SGP retrieved τ , r_e are from the standard ARM algorithm, which combines microwave-radiometer and solar-radiometer measurements. Overall, τ retrievals from VIRS and MODIS had about a -4% bias with respect to the ground-based retrievals, while r_e retrievals showed biases of +8% and -14%, respectively. The satellite

LWP retrievals had biases varying from +16% to -18%, while instantaneous differences were on the order of 50%. However, these biases should not be equated with error, as the ground based retrievals have a significant uncertainty as well.

Minnis then presented LWP comparisons between VIRS and TMI. The regressions were categorized according to the likelihood that the observed VIRS water cloud was part of a multilayer scene (i.e., probably single layer, probably multilayer, and an intermediate determination), with the scene-type metric being the difference between the IR cloud temperature and the effective cloud temperature as derived from the microwave retrieval. Plots of LWP vs. various quantities (τ , SST, surface-wind speed, water vapor, sun-glint potential, solar and viewing zenith angle, and scattering angle) were generated for VIRS and TMI multi-month retrievals and separated according to the three scene types. In general, the observed tendencies were dependent on scene type as expected. There was some correlation with scattering angle, but no tendencies vs. viewing angle or sunglint. No significant differences were found as a function of solar zenith angle for angles less than 70°. The biases are minimal for all categories when the TMI cloud water temperature is between 265-290 K, while TMI LWP is less than the VIRS values for temperatures outside this range. The bias for the cold clouds may be due to uncertainties in the microwave absorption coefficients for supercooled water and/or the presence of ice. Larger biases/tendencies seen in the multilayer and intermediate cloud scenes (e.g., no water detected by TMI despite large VIRS optical thickness retrievals) may be due to TMI detection problems or VIRS retrieval errors.

Comparisons between GOES retrievals at the ARM sites suggest that the CERES method produces an overestimate of LWP when the microwave retrievals are very large because the imager retrievals are less representative of the cloud column when the cloud is very thick. A simple correction can be developed to improve the correspondence between the two data sets. Considerable uncertainty still remains in the microwave retrievals for large values of LWP, a condition that often includes drizzle.

Future efforts will include further work with the Aqua AMSR-E and additional surface-based microwave retrievals and comparison with the MODIS MOD06 and MOD08 (Level 3 aggregation) products.

Combined Satellite Microwave, Visible and Infrared Measurements

Bing Lin from NASA LaRC discussed the synergy between imager and microwave water path data sets, including issues involved in combining the observations, example results, and related activities in the CERES group.

Lin described the algorithms that make use of combined VIRS/TMI and MODIS/AMSR-E data sets. The imager is used for cloud masking and cloud retrievals (τ , r_e , LWP, IWP) as described by Minnis, while his own microwave observations provide LWP and effective water cloud temperature (T_w). He began by noting that microwave brightness temperature has a near-linear relationship with LWP, but is less sensitive than imager observations. Because of this reduced sensitivity, coupled with large uncertainties in cloud water and water vapor continuum absorption, Lin uses imager clear-sky observations to tune his

microwave radiative transfer model so that calculated brightness temperatures are consistent with the microwave observations. He noted that the microwave water absorption coefficient is a strong function of temperature (decreases with temperature) but is not accounted for in most current retrieval algorithms.

Lin summarized comparisons from VIRS and his TMI LWP retrievals. For warm clouds in July 1998, the bias was ~ 0.005 mm, with an RMS difference of ~ 0.03 mm (from analysis of 1° gridded TRMM data). The two techniques showed a similar zonal pattern. A combination of the microwave and imager techniques allows for the inference of multilayer cloud scenes, e.g., ice cloud overlying water cloud. For cold clouds, the VIRS zonal water path was significantly larger than the TMI LWP, indicating the effect of upper-level ice clouds. For such multilayer scenes, the difference between the VIRS retrieved ice water path (IWP) and the TMI LWP approximates the actual column IWP. This estimate for the inferred zonal IWP was found to agree well with zonal VIRS retrievals aggregated only for observations where TMI reported no water cloud. Lin also discussed the LaRC AMSR-E microwave LWP retrievals, along with the AMSR-E standard product. Comparisons between the LaRC retrievals and AMSR-E product show a difference of about 0.01 mm.

A new algorithm has been developed for an ice cloud overlying a water cloud, using a combination of microwave and imager data, to infer separately ice cloud properties (IWP, τ , r_e) and water cloud properties (LWP, r_e , T_w). The combined algorithm (which has only been applied to TRMM VIRS and TMI so far) first determines the water cloud properties from the microwave observation and then iterates on the ice cloud properties until calcu-

lated VIRS radiances are consistent with the imager observations. This algorithm was compared with microwave radar (the Millimeter Cloud Radar, MMCR) retrievals of IWP at the ARM SGP site for 8 multilayer/phase scenes. Compared with the imager-only retrievals, the combined algorithm reduced the retrieved ice cloud optical thicknesses and IWP, as expected. IWP from the combined algorithm compared favorably with the radar retrievals. Histograms of IWP from the imager-only and combined algorithm were collected for SGP-observed multilayer scenes for half a year. The mean IWP and ice-cloud optical thickness from the combined algorithm were about 20% and 24% less, respectively, than means from the imager retrieval. For the combined algorithm, the changes in ice-particle effective size were small ($\sim 7\%$ larger for the combined algorithm). Finally, Lin discussed the detection of drizzle and light precipitation, noting that comparison of the effective radius from the combined algorithm and the imager-only algorithm has potential for this purpose. This is an on-going research effort and *in situ* validation is needed.

Session 2b: Aqua Cloud Retrievals: Cloud-Top Properties

Chair: Steve Platnick, NASA GSFC

AIRS Cloud-Clearing and Cloud-Top Properties

Joel Susskind of NASA GSFC gave an update on the AIRS cloud-top properties product, beginning with a general overview of the AIRS cloud-clearing algorithm. In the sounder context, *cloud clearing* is synonymous with understanding how clouds impact scene radiances and not necessarily the elimination of cloud-contaminated AIRS observations. Initial cloud clearing is done with AMSU microwave radiometer ob-

servations. The cloud products include cloud-top pressure (p_c) and effective cloud fraction (the product of the true fraction and cloud emissivity). Various quality control flags (stratospheric and tropospheric temperature tests, SST tests, etc.) are applied to the clear and cloudy sky retrievals. The percentage of retrievals that pass the various quality tests as a function of effective cloud fraction were shown. Clear-sky profile and surface-parameter retrievals are typically produced for locations with up to 90% cloud cover.

The validation of AIRS cloud retrievals has recently included comparisons with the MODIS Level 2 and Level 3 cloud products (MYD06/MYD08). The MODIS product uses a CO₂ slicing algorithm for mid-to-upper-level clouds, similar to AIRS. Global images and zonal means of cloud fraction and cloud-top pressure from January 2003 and 2004 were shown. In all latitude bands, AIRS cloud fraction means are smaller than the MODIS means, as are the AIRS cloud-top pressure means (indicating higher altitude cloud tops relative to MODIS). The cause of the discrepancy is not known and will require further study. However, inter-annual variability of AIRS is similar to MODIS. The outgoing longwave radiation (OLR) product, which is sensitive to cloud properties and their distribution, was compared with CERES results and found to match well, showing a small bias. The inter-annual difference in monthly mean OLR between January 2004 and January 2003 derived from AIRS was virtually identical to the difference derived from CERES.

Susskind concluded by stating that the new version 4.0 algorithm, which will be delivered to the GSFC Earth

Sciences DAAC shortly, will be used for all forward processing as well as the re-processing of all AIRS/AMSU data back to September 2002. He will recommend that HSB not be used in the re-processing, in order to maintain continuity in the product data set for climatological purposes.

AIRS/MODIS Cloud-Top Property and Cloud-Clearing Activities at CIMSS

Allen Huang from the Cooperative Institute for Meteorological Satellite Services (CIMSS) at the University of Wisconsin, presented the next talk on behalf of **Jun Li** (also of CIMSS), who was unable to attend. A number of efforts have been underway at CIMSS to explore methods for combining MODIS imager and AIRS sounding data, as reported by Li *et al.* in three 2004 publications. Examples from cloud-clearing and cloud-top property activities were reported.

The talk began with an overview describing use of MODIS high resolution imagery to provide AIRS sub-pixel cloud information (cloud masking, cloud phase, cloud-top pressure, and a multilayer cloud assessment). The algorithm begins with an aggregated MODIS product that provides the number of MODIS clear sky confidence pixels in each AIRS footprint. An example was shown of Hurricane Isabel's approach to the east coast of the U.S. on 17 September 2003, with the MODIS cloud classification mask superimposed onto AIRS footprints, indicating those AIRS pixels with mixed cloud layers from MODIS cloud classification. The example was presented to demonstrate that MODIS can be used as a quality check for AMSU/AIRS cloud-clearing or used directly as part of a cloud-clearing scheme.

A second effort at CIMSS has been to perform cloud property retrievals from AIRS radiances. Two approaches have been taken: a one-dimensional variational approach using MODIS cloud products as the *a priori* state, and the Minimum Residual (MR) algorithm that uses only AIRS radiances. Both approaches use MODIS cloud mask and phase information. Examples of these two types of AIRS retrievals were shown for cloud-top pressure and compared with the MODIS results as well as GOES sounder retrievals. Both AIRS retrievals compared well with the other instruments. It was concluded that the AIRS algorithms provided better cloud-top pressure than MODIS for low clouds. The information content of AIRS data for retrieving optical thickness and effective particle size for relatively thin ice clouds was discussed next. Particle size information is derived from the shape of the brightness temperature vs. wavenumber curve in the 800-1000 cm⁻¹ window. Huang pointed out the importance of having continuous spectra throughout this spectral region and discussed how discontinuities in the spectra, e.g., detector array misalignment, can be problematic. Members from the AIRS team stated that the AIRS L1B data file has a quality indicator referred to as the Cij quality flag that is used to indicate channel alignment issues. Returning to the Hurricane Isabel observation, an example of the AIRS cloud optical thickness retrieval from the MR algorithm was shown and compared with MODIS. AIRS tended to underestimate the MODIS solar algorithm (MOD06/MYD06), likely suggesting lower-level cloud layers, but obtained a higher occurrence of thin cirrus ($\tau < 1$), indicating its sensitivity in this part of the retrieval space. While the advantage of the AIRS retrieval is that it can be done

for both day and night observations, it is not useful for relatively thick clouds, i.e., τ greater than ~ 4 , where IR radiances saturate.

Cloud-Assimilation Activities at GSFC GMAO

Peter Norris of the University of Maryland Baltimore County Goddard Earth Sciences and Technology (UMBC GEST) center presented an overview of recent cloud data assimilation activities at the GSFC Global Modeling and Assimilation Office (GMAO). Norris explained the different approaches to the relatively new field of cloud data assimilation. These include: (1) direct assimilation of cloudy radiances; (2) use of cloud observations in diagnostic models to generate or augment model relative humidity (RH) consistent with a model's RH-based cloud parameterization; or (3) data-driven estimation of the empirical parameters of a model's diagnostic cloud parameterization (with no change in the RH analysis). The latter parameter estimation approach has recently been adopted as part of a research effort at GMAO. The GMAO GEOS-4 model uses the CCM3 diagnostic cloud fraction parameterization. Using the parameter estimation methodology, modeled cloud properties are driven towards cloud observations by modifying those empirical cloud parameters related to sub-grid variability and cloud overlap.

Norris then described the cloud data sets that have been considered for assimilation: cloud cover, cloud-top pressure, and cloud optical thickness from ISCCP and MODIS, and cloud liquid water path from SSM/I and MODIS. As an example, Norris showed a considerable improvement in model zonal longwave cloud forc-

ing (as compared with independent CERES data) when assimilating ISCCP cloud fraction alone. He then showed further improvements with the additional assimilation of SSM/I LWP and ISCCP cloud optical thickness. Finally he showed that the best results to date were obtained for recent MODIS Terra and SSM/I assimilations. These produced significant improvements in both longwave and shortwave cloud forcing.

Norris concluded by discussing future efforts which are expected to include modification of the assimilation algorithm for use with the new statistical-prognostic cloud parameterization in GEOS-5, and use of other MODIS cloud retrievals (water path, effective radius) and AMSR-E LWP.

Session 3: Aqua Water Vapor Validation

Chair: Mous Chahine, NASA JPL

The third and final session of the meeting was chaired by AIRS Science Team Leader Mous Chahine and focused on validation (especially water vapor validation), including presentations on validation efforts by the AIRS, MODIS, and AMSR-E science teams. After a brief introduction, Chahine showed a matrix of validation sources and Aqua water vapor data products. He then introduced Eric Fetzer to begin the presentations.

Validation and Science Analyses of AIRS Water and Other Quantities

Eric Fetzer of NASA JPL began by stating the unified nature of the AIRS/AMSU products. Compared to dedicated radiosondes, AIRS/AMSU is achieving 1-K accuracies in 1-km layers of the atmosphere at oceanic sites and is achieving 15% absolute humidity ac-

curacies in 2-km thick layers. However, caution should be used when drawing conclusions at highly variable sites, such as the ARM Southern Great Plains (SGP) site and the Chesapeake Light Platform. AIRS/AMSU water vapor profiles are available globally under both cloudy and clear conditions.

Fetzer then commented on the tropical and mid-latitude oceanic differences between the AIRS/AMSU and AMSR-E total water vapor products. AMSR-E and AIRS/AMSU total water are highly correlated for full and microwave-only AIRS/AMSU retrievals, but AIRS/AMSU is wetter than AMSR-E by approximately 0.4 mm precipitable water at night (approximately a 1% bias). Lastly, Fetzer noted that in diagnosing the effects of clouds, errors in AIRS retrievals are scene-dependent and over-ocean scene variability is dominated by clouds. MODIS will play a key role in cross-validation with AIRS clouds.

Comparison of AIRS and Aura-MLS Upper Tropospheric Water Vapor

The next presentation was also given by Fetzer, this time on behalf of Bill Read from NASA JPL, and concerned the results of the Microwave Limb Sounder (MLS). Fetzer showed a comparison of MLS, AIRS/AMSU, and the GSFC GMAO water vapor at 215 mb. AIRS and MLS are in reasonable agreement.

Fetzer then showed preliminary results of MLS-AIRS/AMSU Upper Tropospheric Water Vapor (UTWV) percent difference in zonal means and a comparison of AIRS and MLS temperature and upper tropospheric clouds. He pointed out that high precision and accuracy require careful point-by-point comparisons and that the means of dif-

ferences should be considered, not the differences of the means. Additionally, care should be exercised when comparing dissimilar fields, for example MLS cloud-ice properties and AIRS/AMSU cloud-height dependence.

Aqua Validation Activities using Raman Lidar and Radiosondes including the AIRS Water Vapor Experiment (AWEX) field campaign

David Whiteman from NASA GSFC reviewed some of the early AIRS/AMSU water vapor validation results, including measurements that occurred in the fall of 2002 at GSFC. The water vapor measurements were gathered by the Scanning Raman Lidar (SRL), and corresponding temperature and pressure measurements were gathered by the Sippican radiosonde. Discrepancies between AIRS/AMSU observations and calculated radiances based on these and other measurements acquired during the early stages of the Aqua validation effort helped to motivate the AIRS Water Vapor Experiment (AWEX), which was conducted October 27 - November 19, 2003 at the U.S. Department of Energy Southern Great Plains site in northern Oklahoma. A total of 56 balloons and 112 sonde packages were launched during AWEX, with the goals of comparing radiosonde and Raman lidar instruments in use for Aqua and developing algorithms for increasing the accuracy of both radiosonde and Raman lidar measurements. AWEX measurements have been used to develop new corrections to the Vaisala RS-80 and RS-90/92 radiosondes that result in significantly improved agreement of these sensors with the AWEX reference sensor—the University of Colorado Cryogenic Frostpoint Hygrometer (CU-CFH). In addition, new correc-

tion techniques were developed for the Raman lidar that address the influence of both the lidar overlap function and the temperature dependence of Raman scattering on the calibration of the water vapor mixing ratio. After all the corrections were applied to both the Vaisala radiosondes and the Scanning Raman Lidar (SRL) data, agreement in mean tropospheric calibration of $\pm 5\%$ was achieved for these water vapor profiling systems with respect to CU-CFH. Corrected versions of the special Vaisala RS-90 radiosonde measurements acquired at the ARM sites have been supplied to the Aqua validation effort for use by other Aqua investigators. Updated versions of the fall 2002 SRL data have also been supplied to the data archive.

Column Water Vapor Retrievals from MODIS Near-IR Channels

Bo-Cai Gao from the Naval Research Laboratories (NRL) provided a brief history on the MODIS near-IR channels for water vapor retrievals, noting that the use of the five channels located near $1 \mu\text{m}$ was largely based on the analysis of hyperspectral imaging data collected with the NASA JPL Airborne Visible/InfraRed Imaging Spectrometer (AVIRIS) instrument during the late 1990s. He then went on to describe the MODIS near-IR water vapor algorithm.

Gao illustrated ratio techniques for water vapor retrievals from MODIS near-IR channels and presented sample retrieval results from both the Terra and Aqua MODIS data, under cloud-free conditions. He compared MODIS near-IR water vapor values with ground-based upward-looking microwave-radiometer measurements of water vapor for validation purposes, demonstrating that by combining the

MODIS near-IR water vapor data over land and the SSM/I water vapor data over water surfaces, a significantly improved water vapor product with nearly global coverage can be produced. Such products can be very useful for climate-related research.

Microwave Water Vapor Retrievals from AMSR-E

Frank Wentz from Remote Sensing Systems gave a presentation on the validation of the AMSR-E water vapor retrievals over oceans. The first part of the validation involved comparing the AMSR-E retrievals to similar retrievals derived from the TMI and from the three SSM/I instruments currently in orbit. The results were displayed as scatter plots in the form of joint probability distribution functions: the vapor difference of AMSR-E minus MI vs. MI vapor, where MI denotes either TMI or SSM/I, depending on the plot. The agreement between the various satellite vapor retrievals is on the order of 0.5 mm. On average, no significant biasing was detected between the AMSR-E water vapor retrievals and the other satellite retrievals.

Wentz compared the diurnal cycle of water vapor over the world's oceans with the cloud water diurnal cycle. The water vapor showed little systematic change with local time of day. In contrast, the cloud water exhibited a very strong diurnal variation, reaching maximum values near 6:00 a.m. and then drying out and reaching a minimum value near 3:00 p.m. Certain areas, such as off the west coast of Peru, showed a markedly strong cloud signal.

One important component of the validation of water vapor relates to the generation of climate time series. Water vapor

is the primary greenhouse gas in the atmosphere. It is responsible for 60% of the greenhouse effect, followed by CO₂ at 25% and O₃ at 8%. Water vapor is also a useful proxy for the air temperature in the lower troposphere. The signal-to-noise characteristics of the water vapor retrieval are considerably better than those for the lower troposphere temperature retrievals done with AMSU. In view of the importance of water vapor to climate studies, a very careful intercalibration of AMSR-E with TMI and the SSM/I sensors is being carried out.

Finally, Wentz discussed a new scientific application for the microwave vapor retrievals, i.e., the determination of the horizontal advection of water vapor. There are currently nine satellite microwave radiometers in low-Earth orbit, all capable of imaging the total content of water vapor in the atmosphere. With this many satellites in orbit at one time, feature tracking can be done, similar to the feature tracking done from geostationary images of cloud motion and upper-level water vapor motion. By tracking the total water vapor content, as opposed to just upper-level vapor, researchers can determine the horizontal advection of water vapor in the atmosphere. This is a critical term in balancing the precipitation-evaporation (P-E) equation. Coupled with an estimate of evaporation, the determination of the horizontal advection of water vapor provides a new and independent means of estimating monthly precipitation over the oceans.

MODIS Infrared Atmospheric Profiles and Water Vapor Updates

Jun Li from CIMSS at the University of Wisconsin-Madison was unable to attend the workshop but submitted his presentation electronically. The submit-

ted presentation included updates of the MODIS water vapor product and gave an overview of the spectral and spatial characteristics of the MODIS infrared atmospheric products. These products are available under cloud-free conditions only. Recent updates to the algorithms have been implemented, including performing saturation checks of profiles, improved surface characterization of each profile (new emissivity and skin temperature), and regression-based ozone profiles for areas where ozone originally was not available. Also, new land/ocean partitionings of training data and retrievals were completed to take advantage of new and more physical emissivity and skin temperature. Other changes include modified zones to allow for sufficient profiles after partitioning into land and ocean groups and the application of destriping to Level 1B prior to performing the retrievals. The resulting improvements include the reduction of the moist bias for dry cases, reducing the along-track noise with the improved training data, improved polar ozone, and the reduction of across-track striping.

The new algorithm makes significant improvements in Aqua image quality, reducing along-track noise and splotchiness due to surface effects. Aqua MODIS has better quality than Terra MODIS for total precipitable water vapor and ozone; but a good global training data set that contains physically realistic surface emissivity and surface skin temperature is crucial for MODIS IR atmospheric products.

GPS/ACARS Comparisons

Larry McMillin of NOAA/NESDIS described comparisons of AIRS moisture with GPS and radiosondes. He noted

that GPS only gives Integrated Precipitable Water (IPW) while both the AIRS and radiosondes provide profiles. Because the GPS observations are continuous and AIRS and radiosondes are not, cases with large changes in GPS IPW between the AIRS observation times are discarded. Once the data are screened, two types of comparisons are made. In the first, total water vapor amounts from all three sensors are compared. The GPS vs. radiosondes had the best fit, but only by a small amount; AIRS compares well with both profiles.

In the second comparison, the GPS data were used to adjust the radiosondes for the sonde-to-sonde calibration errors and the ratio of the GPS IPW to the AIRS IPW was used to adjust all the layer water vapor amounts from the radiosondes. The layer amounts from AIRS and the radiosondes were then compared. In essence, the GPS was used to adjust the radiosondes, AIRS was used as an independent data source to validate the procedure, and the adjusted radiosonde values were used to validate the AIRS. The procedure produces a more accurate validation source for AIRS. A GPS station at each radiosonde site can provide a significant increase in accuracy.

Following the moisture comparisons, temperature comparisons with aircraft observations from September 2002 were shown. All reports within 100 km of fixed aircraft sites in the U.S. and Europe were included as part of a profile and were matched with JPL AIRS temperature profiles. For each site profile, the AIRS temperature was interpolated to the Aircraft Communication Addressing and Reporting System (ACARS) pressure and recorded, and scatter and difference plots when created. Moisture is also measured

and reported by many of the aircraft, but the current sensors have calibration issues, which must be removed by extensive post processing. As a result, the real-time values are mostly rejected by quality-control procedures. A new sensor has been developed and tested, but deployment has been slow. When available, it will provide a reliable source of moisture information in the upper atmosphere, where radiosondes have problems. At the present time, only a few moisture reports are now passing checks.

Overall, there is good agreement of the AIRS measurements with GPS and radiosondes, but there is a slight tendency for AIRS to indicate a wetter atmosphere under the driest conditions and a drier atmosphere under the wettest conditions.

Assimilation of Total-Column Precipitable Water Vapor and Rain Rate Data from Microwave Radiometers

The last formal presentation of the meeting was given by **Toshiharu Tauchi** of JMA's Numerical Prediction Division. Tauchi gave a brief overview of the JMA numerical weather prediction models and assimilation systems and showed a flow chart regarding the general flow of microwave radiometer assimilation. JMA has been incorporating SSM/I and TMI Level 1B data into their operational mesoscale models since October 2003.

Total Column Precipitable Water (TCPW) is being assimilated into the Global 3D-Var model. Positive impacts include better cloud-distribution, rainfall, and typhoon-track forecasts. Negative impacts include a conflict with a model-originated cooling bias in the mid-range forecasts.

MicroWave Radiometer Rain Rate (MWR-RR) data are being assimilated as hourly accumulated precipitation data into the Meso 4D model. The change brought by the rain rate assimilation was to adjust the large-scale condensation into the MWR-RR.

With respect to the impacts of AMSR-E data, better coverage and the ability to directly receive the data at JAXA's Earth Observation Center (EOC) are clearly beneficial. These data have been available since July 2004 and are received and processed at JAXA/EOC and distributed within 30 minutes. Verification studies have been undertaken for both summer and winter scenarios, including a heavy rain event that occurred in Fukui on July 17, 2004. Rainfall verification showed the threat score for heavy rain had been improved at almost all forecast times.

In addition to SSM/I and TMI data, AMSR-E data work well for some experiments with the mesoscale model, and there are plans to introduce the AMSR-E data assimilation system into mesoscale analysis in November 2004.

Open Discussion on Assimilation of Water Vapor Data into GCMs

The presentation by Tauchi was followed by a general discussion on water vapor assimilation by GCMs. **Bob Atlas** of GSFC described his experience with water vapor assimilation and pointed out shortcomings in modeling that lead to a negative impact on simulation results, even when perfect water vapor data were assimilated. **Chris Barnett** of NOAA/NESDIS showed plans by John Le Marshall of JCSDA to begin studies on the assimilation of water vapor into the NCEP model. There was a consen-

sus that much more fundamental work is still needed in this area.

Recommendations

Chahine explained that a central objective of these Aqua workshops is to achieve a consensus on the accuracies of selected Aqua data products. He referred back to last year's Aqua workshop on SST as a model. (The minutes for the Aqua SST workshop are available in *The Earth Observer*, vol. 15, no. 4, pp. 3-18, 2003.) This current workshop has started the process for atmospheric water vapor, but more work remains to be done.

The session ended with a discussion of a set of recommendations laid out by Chahine and further efforts needed for the validation of Aqua water vapor data. Key points included:

- One month should be selected for comparison of water vapor products from AIRS, AMSR-E, and MODIS.
- George Aumann** volunteered to arrange this.
- An urgent need exists for "accurate" upper-tropospheric water vapor data, for validation of the Aqua water vapor products
- Important differences exist between radiative transfer models of the water vapor band used by different numerical weather prediction centers. This remains an issue among users of Aqua products.
- There is a need for understanding/explaining the differences between the cloud products (effective cloud amount and effective cloud-top heights) derived from the AIRS and MODIS measurements.
- The possibility of deriving boundary layer water vapor from the Aqua instruments should be explored.

Acronyms

ACARS: Aircraft Communication Addressing and Reporting System
 ADM: Angular distribution model
 AIRS: Atmospheric Infrared Sounder
 AMSR-E: Advanced Microwave Scanning Radiometer for EOS
 AMSU: Advanced Microwave Sounding Unit
 ARM: Atmospheric Radiation Measurement
 AVIRIS: Airborne Visible/InfraRed Imaging Spectrometer
 CALIPSO: Cloud-Aerosol Lidar and Infrared Pathfinder Satellite Observations
 CERES: Clouds and the Earth's Radiant Energy System
 CIMSS: Cooperative Institute for Meteorological Satellite Services
 DAAC: Distributed Active Archive Center
 EOC: Earth Observation Center
 EOS: Earth Observing System
 ERB: Earth Radiation Budget
 ERBE: Earth Radiation Budget Experiment
 ERBS: Earth Radiation Budget Satellite
 GCM: Global Climate Model
 GLAS: Geoscience Laser Altimeter System
 GMAO: Global Modeling and Assimilation Office
 GOES: Geostationary Operational Environmental Satellite
 GPS: Global Positioning System
 GSFC: Goddard Space Flight Center
 HIRDLS: High Resolution Dynamics Limb Sounder
 HSB: Humidity Sounder for Brazil
 ICESat: Ice, Cloud, and land Elevation Satellite
 IEEE: Institute of Electrical and Electronics Engineers
 IPW: Integrated Precipitable Water
 IR: Infrared
 ISCCP: International Satellite Cloud Climatology Project
 IWP: Ice water path
 JAXA: Japan Aerospace Exploration Agency

JMA: Japan Meteorological Agency
 JPL: Jet Propulsion Laboratory
 JCSDA: Joint Center for Satellite Data Assimilation
 LaRC: Langley Research Center
 LWP: Liquid Water Path
 MIT: Massachusetts Institute of Technology
 MLS: Microwave Limb Sounder
 MODIS: Moderate Resolution Imaging Spectroradiometer
 MOPITT: Measurements of Pollution In The Troposphere
 MR: Minimum Residual
 MWR-RR: MicroWave Radiometer Rain Rate
 NCEP: National Centers for Environmental Prediction
 NESDIS: National Environmental Satellite, Data, and Information Service
 NOAA: National Oceanic and Atmospheric Administration
 NPOESS: National Polar-orbiting Operational Environmental Satellite System
 NPP: NPOESS Preparatory Project
 OCO: Orbiting Carbon Observatory
 OLR: Outgoing longwave radiation
 OMI: Ozone Monitoring Instrument

PARASOL: Polarization and Anisotropy of Reflectances for Atmospheric Sciences coupled with Observations from a Lidar
 PDF: Probability distribution function
 RAOB: Radiosonde observation
 RH: Relative humidity
 RMS: Root mean square
 RSS: Remote Sensing Systems
 SGP: Southern Great Plains
 SSM/I: Special Sensor Microwave/Imager
 TCPW: Total Column Precipitable Water
 TES: Tropospheric Emission Spectrometer
 TGARS: Transactions on Geoscience and Remote Sensing
 TMI: TRMM Microwave Imager
 TOA: Top of the atmosphere
 TOMS: Total Ozone Mapping Spectrometer
 TRMM: Tropical Rainfall Measuring Mission
 TWP: Tropical Western Pacific
 UMBC GEST: University of Maryland Baltimore County Goddard Earth Sciences and Technology
 VIRS: Visible and Infrared Scanner



Kudos

For the first time, NASA researchers have been awarded the Scientific American Top 50 Scientist Award. Climatologists **Drew Shindell** and **Gavin Schmidt**, NASA's Goddard Institute for Space Studies (GISS), New York, recently received the award given by *Scientific American Magazine*.

The Scientific American 50 is a prestigious annual list, published in the December edition, recognizing outstanding acts of leadership in science and technology from the past year. Shindell and Schmidt were named Research Leaders in the Environmental Studies for seeking clues in the global warming category.

The Earth Observer staff and the entire EOS community congratulate Shindell and Schmidt on this outstanding accomplishment.

Pathfinding for EOS Product Data Format Transition From HDF-EOS2 to HDF-EOS5

— Zhangshi Yin, yin@killians.gsfc.nasa.gov, Global Science & Technology, Inc
 — Jingli Yang, jyang@ertcorp.com, Earth Resources Technology, Inc
 — Rich Ullman, Richard.E.Ullman@nasa.gov, Goddard Space and Flight Center, NASA

Introduction

NASA selected the Hierarchical Data Format (HDF) as the standard data format to use for the Earth Observing System (EOS) program when it began back in 1993. HDF is a package of software, libraries, and tools for analyzing, visualizing, and converting scientific data. HDF is an important component for EOS missions, which bring back massive amounts of data each day. HDF allows users to move and share data regardless of the computing platform they use. HDF can handle visual as well as numerical data and allows scientists to include peripheral information about the data in their datasets. Within HDF files, data can be organized in ways that suit the needs of those who access it. For example, temperature data could be organized in HDF in such a way that a scientist who wants to study temperature data can examine those data over time or at different levels in the atmosphere.

The National Center of Supercomputing Applications (NCSA) created an HDF data-format library. Although HDF offered many advantages, EOS required additional conventions and data types that HDF could not handle. For this reason, NASA funded the creation of a modified version of HDF, known as HDF-EOS, specifically designed to meet the needs of EOS. HDF-EOS essentially serves as an upper layer on the HDF data format that standardizes data

storage information and simplifies data production [1].

HDF and HDF-EOS both went through a series of revisions throughout the 1990s, the latest of which took place in 1999 [2]. At that time, the current version of HDF was version 4.15, which became known as HDF4. Likewise, the current version of HDF-EOS was version 2.28, and became known as HDF-EOS2. Meanwhile, in 1998, NCSA developed a completely different data format for use with the EOS Aura mission, which became known as HDF5. HDF4 and HDF5 are not compatible with one another [3]. The HDF-EOS team developed a version of HDF-EOS that would work with this new data format that became known as HDF-EOS5.

HDF5 and HDF-EOS5 offered many improved features over previous versions of HDF and HDF-EOS [4]. These features included greater storage capacity, higher-speed processing, better modeling capabilities, and the ability to conduct parallel and distributed processing. HDF5 also gave users much more control over how data were stored, e.g., compression, chunking, and parallel Input/Output (I/O) on supercomputers. In addition, HDF5 gave users the ability to do aggregation for large data sets, which had previously not been possible [5].

Since it offers so many advantages over its predecessor, HDF-EOS5 is clearly

the data format for the future. Eventually the HDF-EOS team may wish to discontinue support of HDF-EOS2, and so it needs to begin to migrate archived HDF-EOS2 data over to HDF-EOS5 format. The problem as mentioned before is that HDF4 and HDF5 are not compatible, so this implies that HDF-EOS2 and HDF-EOS5 are similarly not compatible [6]. There is a need to transition from HDF-EOS2 to HDF-EOS5. Data producers and data users are concerned about how smoothly this transition would proceed and what difficulties they might encounter in the process.

This article reports on a pathfinding project aimed at answering this question. It tests how easily the Product Generation Executables (PGEs) from a couple of EOS data products (one from MODIS and one from AIRS/AMSU) created using HDF-EOS2 could be converted into PGEs in HDF-EOS5. It considers questions such as:

- How much effort is involved?
- How accurate is the transition result?
- What is the impact on performance?

As the transition from HDF-EOS2 to HDF-EOS5 takes place, one additional task that needs to be undertaken is to add internal compression to the PGE codes. The EOS data set continues to grow larger every day, and so the need to be able to store compressed

data is very important. HDF and HDF-EOS have built several efficient internal compression functions. Both HDF-EOS2 and HDF-EOS5 support multiple internal compression methods. HDF-EOS2 supports run-length encoding (RLE), skipping Huffman (SKPHUFF), and deflate (DEFLATE) compression techniques. HDF-EOS5 supports DEFLATE and SZIP compression techniques. At present, however, most HDF-EOS2 data products don't have an internal compression function. This function needs to be added to the PGE so that HDF-EOS5 files can be compressed.

Methodology

Data Products

The Moderate Resolution Imaging Spectroradiometer (MODIS) 8-day, Level 3, global, 500-m land-surface reflectance product (MOD09A1) from the Terra satellite was chosen as a test case as was the Atmospheric Infrared Sounder (AIRS)/Advanced Microwave Sounding Unit (AMSU) product (AIRABRAD). These two products are good representative samples of HDF-EOS data; one is gridded data and the other is swath data. The MODIS and AIRS science-data process-

ing teams provided the PGE codes and test data used in the study. They also provided assistance in installation and testing.

A typical **MOD09A1** product has the following format:

Long Name: MODIS/Terra Surface Reflectance 8-day L3 Global 500m SIN Grid
Area: ~10° x 10° lat/long
Image Dimensions: 2 (2400 x 2400 row / column)
Average File Size: 50 – 500 MB
Resolution: 500 m
Projection: Sinusoidal
Data Format: HDF-EOS2

A typical **AIRABRAD** product has the following format:

Long Name: AIRS/Aqua AMSU-A geolocated brightness temperatures
Coverage: Global, twice daily (daytime and nighttime)
Average File Size: 0.45 MB
Resolution: 40.5 km FOV at nadir
Data Format: HDF-EOS2

Procedure

Figure 1 presents a diagram of the procedure that was followed for this

experiment. The PGE package was installed for both products as well as their related libraries such as HDF4, HDF-EOS2, and the Science Data Processing (SDP) tool kit. After testing that the software was installed correctly, the HDF5 and HDF-EOS 5 libraries were added. Once all of the necessary libraries were in place, the first task was to analyze the PGE codes and the relationships between HDF-EOS2 and HDF-EOS5.

One of the most time-consuming tasks in this process was changing the PGE software from HDF-EOS2 Application Programming Interfaces (APIs) to HDF-EOS5 APIs. In addition, data types were changed from HDF-EOS2 to HDF-EOS5, and internal compression functions were added to the PGE codes.

Data-Type Mapping

Data-type flags in HDF-EOS libraries are used to define HDF-EOS2 data-set types. HDF-EOS2 data-type flags are constants, and thus they can be used to define data in data structures. In HDF-EOS5, on the other hand, data-type flags are called identifiers rather than constants. This means that a data-type flag can't be assigned to a data structure. One can only use them in APIs or retrieve them when a program is running. HDF-EOS2 data-type flags are defined by the prefix DFNT, and HDF-EOS5 data-type flags are defined by the prefix H5T_NATIVE. It is easy enough to find mapping relationships between HDF-EOS2 and HDF-EOS5 data-type flags, however. HDF-EOS5 data types need to replace the data types of API arguments. So when creating new APIs, each HDF-EOS2 data type used needs to be transformed to the corresponding HDF-EOS5 data type.

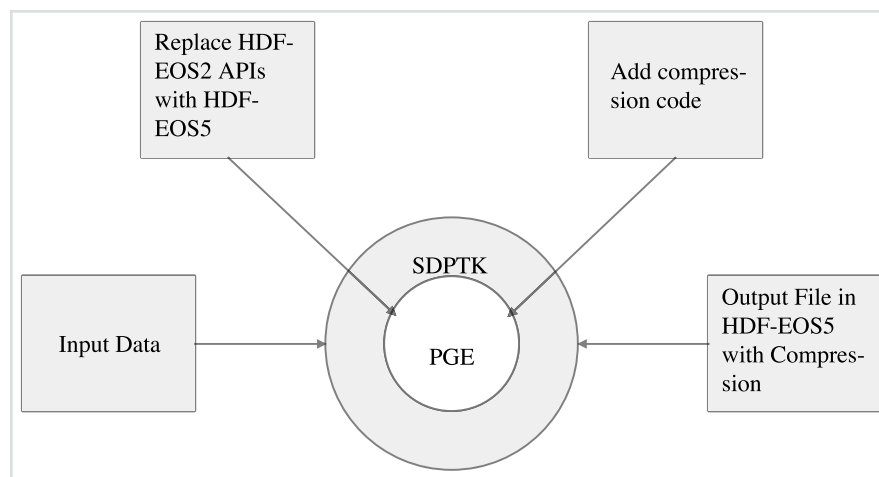
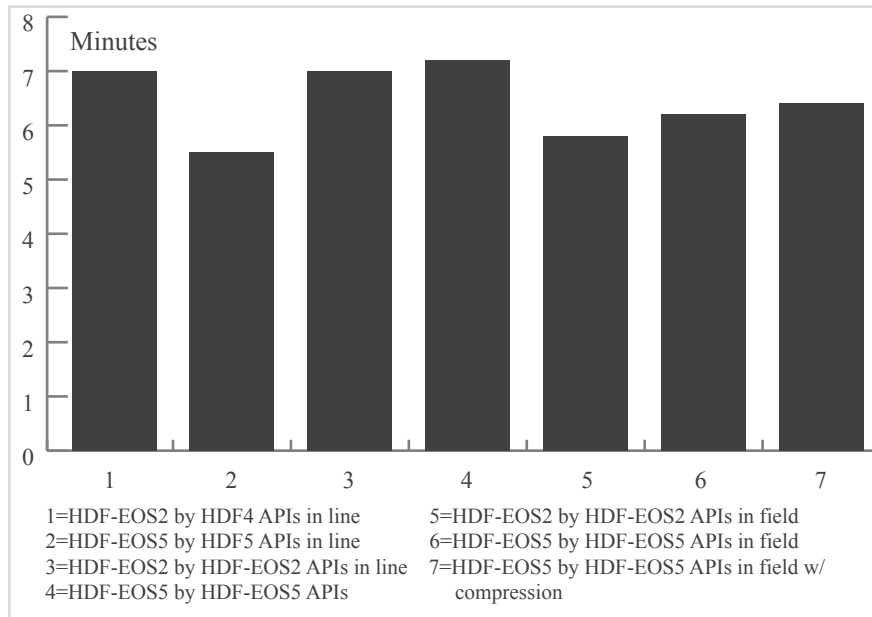


Figure 1: PGE21 Transition from HDF-EOS2 to HDF-EOS5

Figure 2: MODIS Performance Comparison



Data API Mapping

Most APIs that were written in HDF-EOS2 format have corresponding APIs in HDF-EOS5 format. In addition, HDF-EOS5 offers several new APIs. For example, in HDF-EOS5, all levels of file, group, grid, swath, and field are assigned attributes. In contrast, HDF-EOS2 only assigned attributes to grid and swath. In HDF-EOS2, an HDF4 API was needed to deal with the other attributes. So for instance, in the MOD09A1 PGE, the information on calibration would be an HDF4 API. In HDF-EOS5, on the other hand, calibration is handled as a local attribute of an HDF-EOS5 field.

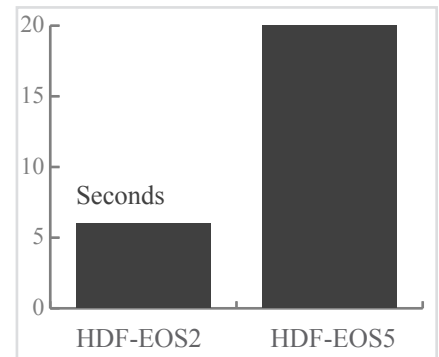
Neither HDF-EOS2 nor HDF-EOS5 have APIs for metadata writing. Meta-

data such as StructMetadata, CoreMetadata, and ArchiveMetadata are handled by using the SDP tool kit.

Adding Compression

In HDF-EOS data compression is only possible when the data are output in fields, not when outputting it line-by-line. Therefore, in order to accommodate data compression capabilities, the file output format has been modified so that it writes out the data by fields rather than line-by-line. Since it is not easy to change the data compression method in the PGE (there is no command line interface), only one compression method was tested as part of this study. The DEFLATE compression method was chosen because it is common to both HDF-EOS2 and HDF-EOS5 and because it is one of the most popular and reliable compression methods.

Figure 3: AIRS Performance Comparison



Results and Testing

After the PGE codes were modified, compiled, and run, HDF-EOS5 data were produced. The MODIS and AIRS HDF-EOS5 product files and metadata files were evaluated. The metadata files can be directly compared with the metadata files before the transition and they turn out to be identical. The product files were tested using several software tools (such as h5view, heex, and h5diff). H5diff shows that HDF-EOS5 images, values, attributes, and metadata are identical to those before the transition. H5view shows that the images are the same as what appeared before the change. This shows that the transition results are accurate and that no information is lost.

Performance

Several different performance tests were conducted. HDF-EOS5 was compared to HDF-EOS2, HDF5 was compared to HDF4, and HDF-EOS5 was compared to HDF5, using both

	Analysis	Visualization	Converter	Data Reader	Subsetter	Projection	Mask	Mosaic	Statistics	Others	Total
HDF4	31	14	5	1	0	0	0	0	0	7	58
HDF5	10	6	4	1	0	0	0	0	0	13	34
HDFEOS2	13	8	9	6	1	3	1	1	1	6	48
HDF-EOS5	1	1	4	0	1	0	0	0	0	2	9

Table 1: HDF and HDF-EOS Software Survey Summary

line-by-line and field outputs. (The field outputs were run both with and without data compression.) The results for the S product are shown in **Figure 2** and for AIRS in **Figure 3**.

From **Figures 2 and 3**, it is clear that there are no significant changes in performance between HDF-EOS2 and HDF-EOS5. The two formats are just about identical when data are output by fields. The only exception is when HDF-EOS5 produces line-by-line output. HDF-EOS5 is about 15 seconds slower than HDF-EOS2. **Figure 2** illustrates that this time differential is fairly trivial for larger, longer-running programs, e.g., the MODIS program that takes 7 minutes to run. However, as **Figure 3** illustrates, with smaller, short-running programs, e.g., the AIRS program that takes 20 seconds to run, the time difference would become quite a bit more noticeable. The HDF-EOS team is aware of this lag time with HDF-EOS5 output and is working to address this issue.

HDF-EOS5 Support Software

Software has been or is being developed to aid in the transition from HDF-EOS2 to HDF-EOS5. The results of a survey of available software are shown in **Table 1**. Survey data was largely provided by NCSA HDF website [6,7] and from the HDF-EOS Tools and Information Center website [8].

Table 1 reveals that there are 58 software tools for HDF4, 34 software tools for HDF5, 48 software tools for HDF-EOS2, and 9 software tools for HDF-EOS5. Software tools have been designed to assist with visualization, conversion, subsetting, projection, validation, importing, reading, writing, storage, and for data serving. The dom-

inant tools for the software are designed for visualization. The government, the education community, and contractors provide most of the software, and most is public domain software. Some commercial companies like Interactive Data Language (IDL) and O-Matrix have already added HDF-EOS5 or HDF5 to their software. MATLAB is also considering developing software to support HDF-EOS5. Other major companies like ESRI, IMAGINE and PCI will also support HDF-EOS5.

The HDF-EOS5 library team and the HDF5 library team have developed HDF-EOS5 and HDF5 visualization tools. ECS has added HDF-EOS5 functions in the Earth Observing System Data and Information System (EOS-DIS) data producing software SDP. As of yet there are few software tools for HDF-EOS5, although basic HDF-EOS5 data support tools are available. These include tools for basic HDF-EOS5 visualization, extraction, conversion, and simple analysis functions. Examples include:

- *For Visualization:* HDFView, HE5View, JEB;
- *For Extraction:* HEEX, HDFView, HE5View;
- *For Conversion:* Hdfeos52netcdf5, heconvert, HEEX, XML2HE.

Conclusions

1. It is feasible to modify PGE software to allow for product transition between HDF-EOS2 and HDF-EOS5.
2. If both the input and output files are HDF-EOS2 objects, e.g., an AIRS PGE, the conversion is fairly straightforward.
3. In input and output files and HDF4 objects and HDF-EOS2 objects, e.g.,

hybrid forms like a MODIS PGE, the modification is do-able, but very time consuming.

4. Performance will depend on many factors. For a large PGE like MODIS, there is not much difference in performance between HDF-EOS2 and HDF-EOS5. On the other hand, for a small PGE like AIRS, the 15-second time differential between HDF-EOS2 and HDF-EOS5 becomes more significant.
5. It is a challenge to develop tools to automate the transition from HDF-EOS2 to HDF-EOS5. Some manual changes will be required.
6. Research efforts will continue to work on developing a better understanding of the program structure and algorithms so that the transformation from HDF-EOS2 to HDF-EOS5 will be easier to accomplish.

Summary

This pathfinding project was designed to test how easy it would be to transition from the HDF-EOS2 data format to the HDF-EOS5 data format. Data from MODIS and AIRS were selected as test cases. The PGE codes were directly modified and analyzed. HDF-EOS2 data types, objects, attributes, and metadata were mapped over to HDF-EOS5. The HDF-EOS2 code was replaced by HDF-EOS5 code (algorithm and data values were kept identical) and internal compression capabilities were added. After the transformation, the new HDF-EOS5 data were tested using h5view, heex, and h5diff. The results show that images, data, attributes, and metadata are identical to what they were before the transformation.

The experiment shows that a transition from HDF-EOS2 to HDF-EOS5 should be feasible. It can be accomplished by modifying the PGEs. The transition result seems to be accurate, and no information is lost during the transformation. The only caveat is that the data take about 15 seconds longer to output in HDF-EOS5 than they did in HDF-EOS2. With large, long-running PGEs like MODIS, this would be an almost negligible difference, but for short, fast-running programs like AIRS, the lag time will be more noticeable.

Acknowledgements

The author wishes to recognize the contributions of the following individuals.

- **Robert Wolfe and Nazmi Saleous** provided MODIS PGE codes, test data, and provided many helpful suggestions.

- **Mike Theobald** provided the AIRS PGE codes, test data, and helped with installation.

- **Evan Manning** provided help with the AIRS PGE installation, debugging, and testing.

References

[1] Schmidt, L. *The Universal Language of HDF-EOS*. earthobservatory.nasa.gov/Study/HDFEOS. December 2000.

[2] Ullman, R. *Status and Plans for HDF-EOS, NASA's Format for EOS Standard Products*. hdfeos.gsfc.nasa.gov/hdfeos/HDFEOS_status/HDFEOSStatus.htm. July 2001.

[3] Mc Grath, R. E, Yang, and Muqun. *Conversion from HDF4 to HDF5: "Hybrid" HDF-EOS Files*. hdf.ncsa.uiuc.edu/h4toh5/Experiment2/heconvert.html. March 2002.

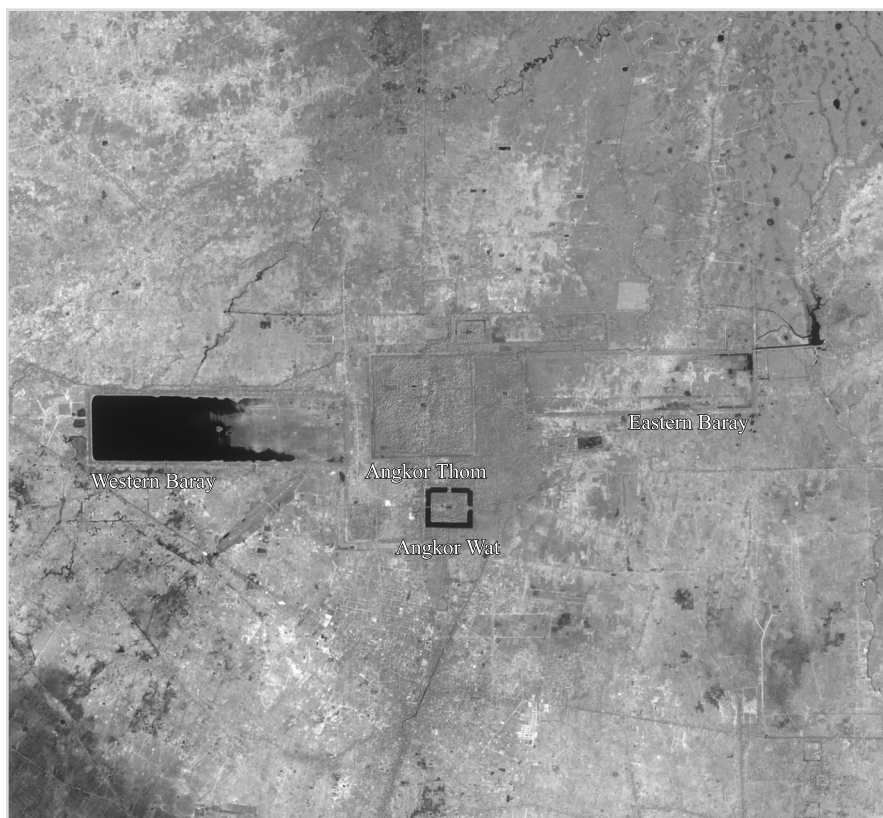
[4] NCSA, *HDF5 for HDF4 Users: A Short Guide*. hdf.ncsa.uiuc.edu/HDF5/papers/papers/h4toh5/HDF5forHDF4Users.pdf. December 2002.

[5] NCSA, *Introduction to HDF5*. hdf.ncsa.uiuc.edu/HDF5/doc/H5.intro.html. October 1998.

[6] NCSA, *Software using HDF4*. hdf.ncsa.uiuc.edu/tools.html. May 2004.

[7] NCSA, *Software using HDF5*. hdf.ncsa.uiuc.edu/tools5.html. May 2004.

[8] *HDF-EOS Tools and Information Center*. hdfeos.gsfc.nasa.gov/hdfeos/softwarelist.cfm. May 2004.



Perhaps the most famous site in Angkor is Angkor Wat, a vast temple complex built by Suryayarman II in the early 12th century to honor the Hindu god Vishnu. The temple complex is clearly visible in this image as the small black frame just below the image center. The frame is created by a 190-meter wide causeway, which encircles three galleries and five central shrines that tower up to 65 meters. The entire complex occupies an area of 1.5 x 1.3 kilometers.

To the north of Angkor Wat is the larger square of Angkor Thom, the inner royal city built in the 12th century. The now dry moat around Angkor Thom is still visible as a pale gray square cut through the surrounding green vegetation. West of Angkor Thom is the vast Western Baray, a reservoir built in the 11th century. The earthen walls constructed to hold water form a perfect rectangle, oriented exactly east-west. Though filled with silt today, the smaller Eastern Baray is also visible in this image. Constructed in the 9th Century, the Eastern Baray was probably about 3 meters deep and held an estimated 37.2 million cubic meters of water.

The image was acquired on February 17, 2004, by the Advanced Spaceborne Thermal Emission and Reflection Radiometer (ASTER) on NASA's Terra satellite. NASA image created by Jesse Allen, Earth Observatory, using data provided courtesy of NASA/GSFC/METI/ERSDAC/JAROS, and the U.S./Japan ASTER Science Team.

AMSR-E SIPS Historical Processing Completed

– Kathryn Regner, *kregner@itsc.uah.edu*, AMSR-E SIPS Systems Engineer

The Science Investigator-led Processing System (SIPS) at the Global Hydrology Climate Center (GHCC), a collaboration between NASA/Marshall Space Flight Center (MSFC) and the University of Alabama in Huntsville, is pleased to announce that historical processing of the entire AMSR-E Level-2B and Level-3 data sets with the latest version of algorithms was completed on October 22, 2004. The AMSR-E data products are provided in both a Level-2, pixel-by-pixel, orbital swath projection and in a Level-3, global space and time averaged (e.g., daily, weekly, or monthly composite) Earth-oriented coordinate grid. These products are available to the public from the NSIDC DAAC nsidc.org/daac/amsr/.

The significance of this processing effort is that it resulted in complete mission datasets using consistent algorithms for each the following products: Level-2 ocean, land, and rain and Level-3 ocean, land, sea ice, snow, and rain from the beginning of the mission through late November. Since the completion of this historical processing activity, the algorithm used to generate Level-3 snow products (global daily, pentad, and monthly granularities) was upgraded to beta version 4. Other products are expected to version up between now and the early summer, when a full reprocessing will begin, which will result in consistent datasets once again. In the mission out years, we expect the algorithms to stabilize and become validated, with reprocessing occurring only once per year or so.

The Advanced Microwave Scanning Radiometer for the Earth Observing System (AMSR-E) is one of the primary instruments flown aboard NASA's Aqua platform, which launched on 4 May 2002. Developed by the Japan Aerospace Exploration Agency (JAXA; formerly NASDA), it improves upon the window frequency radiometer heritage of the Scanning Multichannel Microwave Radiometer (SMMR), Special Sensor Microwave/Imager (SSM/I) and Tropical Rainfall Measuring Mission Microwave Imager (TMI). Major improvements over those instruments include both horizontally and vertically polarized channels spanning the 6.9 GHz to 89 GHz frequency range, and higher spatial resolution from a 1.6 m reflector.

The AMSR-E SIPS is a decentralized, geographically distributed ground-based data processing system comprising two primary components located at Remote Sensing Systems (RSS) in Santa Rosa, California and at the Global Hydrology and Climate Center (GHCC) located within the National Space Science and Technology Center (NSSTC) in Huntsville, Alabama. A core team of personnel, specializing in science data processing, systems administration, data management, software engineering, and systems engineering provides 8 to 5 and after hours on-call project support.

A full reprocessing of the mission data set is planned to begin in early summer of 2005 at the SIPS-GHCC. The regenerated Level-2B and Level-3

products listed above will this time be based upon Level-1A antenna temperature data (reprocessed at JAXA) and Level-2A brightness temperature data (reprocessed at SIPS-RSS), using updated algorithms that improve upon the calibration and geolocation of the instrument data.



Kudos

Veerabhadran Ramanathan, University of California San Diego, and Principal Investigator and Co-Investigator on two EOS proposals, has been appointed an academician of the Pontifical Academy of Sciences by Pope John Paul II. Ramanathan will propose subjects for study and attend scientific meetings, including plenary sessions. He will also nominate outstanding scientists for membership in the organization, and nominate young scientists of international reputation for the Pius XI Medal.

The Earth Observer staff and the EOS scientific community wish to congratulate Dr. Ramanathan on this outstanding achievement.

Earth Science Enterprise Education Program Update

—Ming-Ying Wei, ming-ying.wei-1@nasa.gov, NASA Headquarters

—Diane Schweizer, diane.schweizer@nasa.gov, NASA Headquarters

—Theresa Schwerin, theresa_schwerin@strategies.org, Institute for Global Environmental Strategies

GLOBE PROGRAM GAINS NEW PARTNER FOR STUDENT RESEARCH

France has joined the NASA-sponsored GLOBE program, an international student Earth-science program, to become the 107th country to partner in environmental research worldwide.

The French space agency, Centre National d'Etudes Spatiales (CNES), plans to implement GLOBE in association with the joint US-France Cloud-Aerosol Lidar and Infrared Pathfinder Satellite Observations (CALIPSO) satellite mission, as well as the CNES Polarization and Anisotropy of Reflectances for Atmospheric Sciences coupled with Observations from a Lidar (PARASOL) microsatellite project.

The GLOBE program, established on Earth Day in 1994, enables students to take and report research-quality environmental measurements involving teachers, students, and scientists. It is a hands-on primary and secondary Earth science education program that brings together students, teachers, and scientists to study and research the dynamics of the Earth's environment. Students benefit by improved achievements in science and math. In turn, the research community receives data that generally would not be available if not for the efforts of volunteers. For more information about GLOBE, visit globe.gov.

ODYSSEY OF THE MIND 2005 COMPETITION: GET THE MESSAGE

For the fifth year, NASA is pleased to sponsor an Odyssey of the Mind Long Term Problem. Odyssey of the Mind is an international creative problem-solving program for students from kindergarten to college.

Competing teams in the NASA-sponsored problem—"Get the Message"—will present an original performance that includes a story told three times, each time using a different method of communication: a primitive method, an evolved method, and a futuristic method created by the team. The team will create signals that represent a stage in a process of the Earth system that they will display for each communication method. The presentation will also include a narrator or host and a stage set.

The 2005 World Finals will be held at the University of Colorado in Boulder, May 21-24. For more information, visit www.odysseyofthemind.com.

2005 SUMMER INSTITUTE ON ATMOSPHERIC, HYDROSPHERIC, AND TERRESTRIAL SCIENCES

June 6 - August 12, 2005

Deadline for applications: February 12, 2005

This program is designed to introduce undergraduate students majoring in

all areas of the physical sciences to research opportunities in the atmospheric, hydrospheric, and terrestrial sciences. No previous experience in these sciences is needed. The program is directed primarily at undergraduates who are in their junior year at the time of application. However, all undergraduates, who are currently enrolled in a U.S. college or university, are eligible, provided they are also U.S. Citizens or holders of a Green Card indicating their intention of becoming a citizen.

The first part of the program will be a one-week lecture series, given primarily by NASA Goddard Space Flight Center (GSFC) scientists. The lecture series will be followed by nine weeks of research on topics selected by the students from a suggested list, with a GSFC scientist as a mentor. The program is held at GSFC in Greenbelt, MD, with housing provided at the nearby University of Maryland, College Park. Participants receive a \$3,000 stipend, housing, and the expenses of economy travel. For more information, see: neptune.gsfc.nasa.gov/summerinstitute.

EARTH SCIENCE EDUCATION COMMUNITY MEETING AT ASILOMAR

A community meeting was held November 2-4, in Asilomar, California, to begin envisioning the next decade

of NASA Earth-science education. Meeting participants included 147 representatives of elementary and secondary, higher, and informal education communities from 35 states, the District of Columbia, and Puerto Rico. Information generated by the community during the Asilomar meeting will be the building blocks for developing a roadmap that guides NASA's Earth-science education program for the next ten years.

Alphonso Diaz, Associate Administrator, Science Mission Directorate, provided the keynote address. Forty-one discussion groups focused on 23 topics that were pre-defined by the Earth Science Education Roadmap Steering Committee, as well as topics proposed on-site by community members. Discussion topics ranged from the traditional, e.g., elementary and secondary education, to cross-cutting, e.g., forging alliances and networks, and timely (integrating NASA Earth- and space-science education programs).

Over the next few months, the Earth Science-Education Roadmap Steering Committee will take all the input from the Asilomar meeting and use it to draft the NASA Earth Science Education Roadmap. A spring 2005 community meeting is planned to obtain feedback on the draft roadmap.

The steering committee chair, **Roberta Johnson**, University Corporation for Atmospheric Research, is establishing a Website to post information from the community meeting and the roadmap development. The site will include major plenary presentations, photos, and background information about the conference and the roadmapping process.

NASA leadership for the Earth science education roadmap is provided by **Ming-Ying Wei**, Program Manager, Earth Science Education, and **Paula Coble**, Program Scientist, Earth Science Education.

GLOBE WINS GOLDMAN SACHS FOUNDATION PRIZE

On November 16 the NASA-funded GLOBE Program was presented with a 2004 Goldman Sachs Foundation Prize for Excellence in International Education, for the category "Media and Technology." This prize is awarded to "A private sector or non-profit organization that has developed outstanding programs that use media/technology to educate students or teachers about other world regions and cultures, or international issues."

In June 2003 Asia Society and The Goldman Sachs Foundation created the first Prizes for Excellence in International Education to promote international knowledge and skills in our schools and communities. The program annually awards five prizes of \$25,000 each in the following categories: Elementary/Middle School, High School, State, Higher Education, and Media/Technology.

GLOBE ANNOUNCES 2005 CONFERENCE

The Ninth Annual GLOBE Conference will be held in Prague, Czech Republic, July 31-August 5. The Conference will bring together GLOBE Country Coordinators, U.S. Partnership Coordinators, Education and Science Principal Investigators and others to address key education and science elements. URL: www.globe.gov.

CCAG 2005 EDUCATOR WORKSHOP, HAMPTON, VA

An educator workshop titled NASA Satellites Study Earth's Atmosphere: CALIPSO, CloudSat and Aura working with GLOBE, is scheduled for July 11-20 at Hampton University, Hampton, VA. It targets middle school educators who will work with the missions to involve students in reporting visual cloud observations, ozone, and sun photometer data collection at the GLOBE website. URL: calipsooutreach.hamptonu.edu or contact Barbara Maggi, barbara.maggi@hamptonu.edu.

NEW NASA EARTH OBSERVATORY RSS FEED

The Earth Observatory team announces an RSS 2.0 Specification Feed available. Really Simple Syndication (RSS) is a way of publishing short summaries of what's new on a website, with a link to the actual page should the reader want to know more. URL: earthobservatory.nasa.gov/eo2.rss.

NEW URL FOR NASA'S SCIENCE MISSION DIRECTORATE

As a result of the transformation activities taking place at NASA, the Earth Science and Space Science Enterprises joined to form the Science Mission Directorate. The new URL for the Science Mission Directorate is science.hq.nasa.gov/. Education programs and resources can be found at science.hq.nasa.gov/education.

MY NASA DATA: WORKSHOP FOR REASONING THROUGH THE USE OF EARTH SCIENCE DATA SETS

NASA Langley Research Center will host a hands-on workshop designed for

the 6-12 educator July 25-29. Application deadline is April 8. Earth science teachers are particularly encouraged to apply. The workshop will focus on

the implementation and use of Earth Science data sets developed for student researchers in grades K-12. For more information, visit mydasdata.larc.nasa.gov

or email Joyce Fischer, j.d.fischer@larc.nasa.gov.

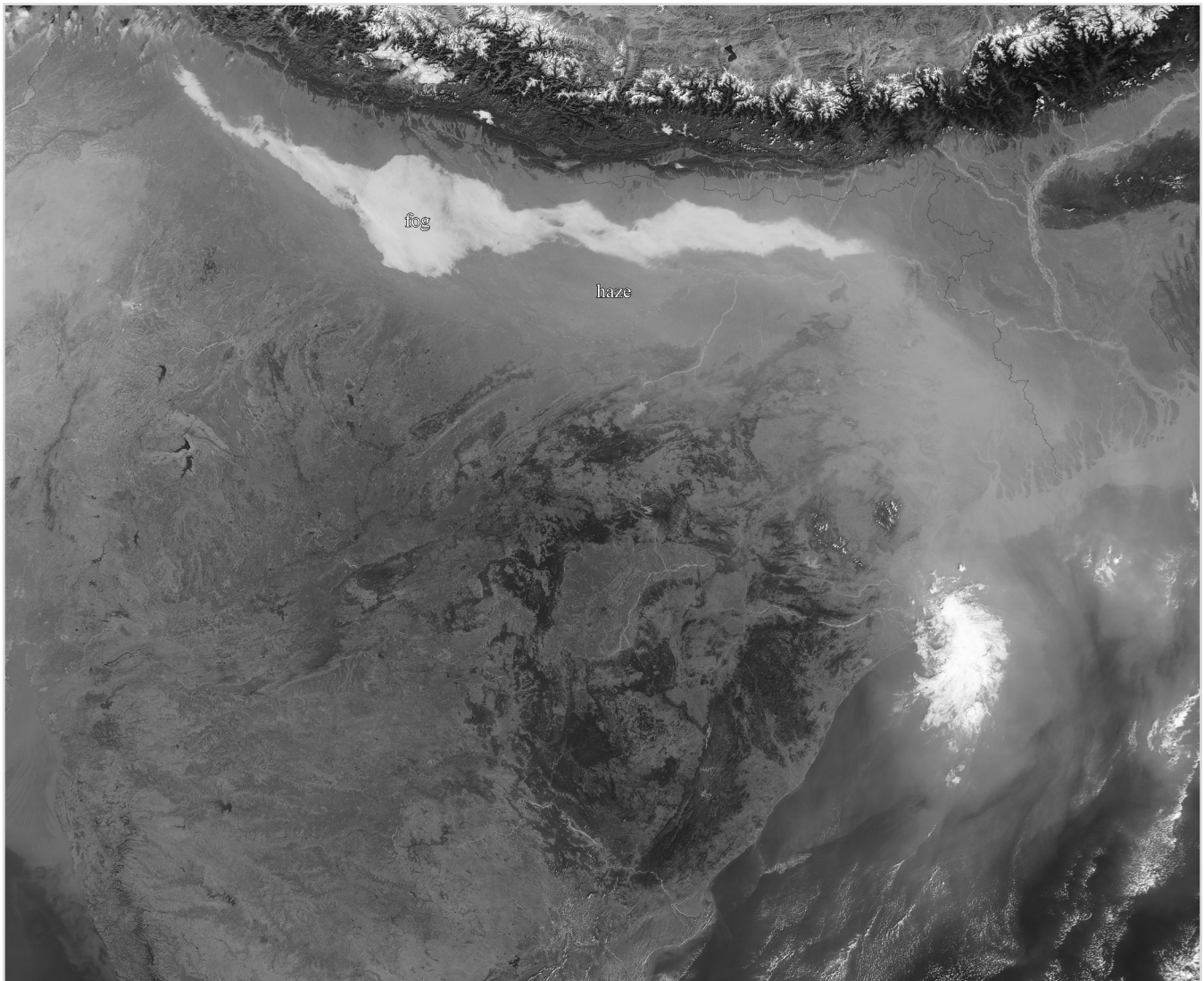


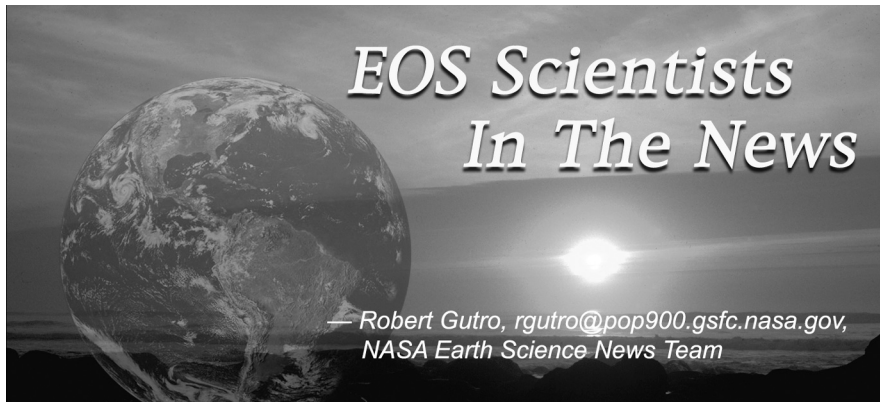
Fog stretched over northern India on December 17, 2004, and mixed with a river of haze that flowed west and south across Bangladesh and over the Bay of Bengal. According to news reports from the area, over the weekend of December 18 and 19, the foggy, smoggy conditions caused numerous deadly accidents in the Indian states of Bihar, Haryana, and Uttar Pradesh. All forms of transportation were delayed throughout the weekend, including air, train, and road traffic.

In this image from the Moderate Resolution Imaging Spectroradiometer (MODIS) on NASA's Terra satellite, India occupies most of the center and left part of the scene, while Bangladesh is located in the upper right quadrant. Haze mingles with the fog at the foothills of the Himalaya Mountains, which arc across the top edge of the image. To the north is a small section of the Tibetan Plateau.

The brightness of the fog is muted by the overlying air pollution. In the lower right corner of the image, the haze stretches out over the Mouths of the Ganges River and onward to the Bay of Bengal. A cloud over the bay appears to be higher in the atmosphere than the haze; its brightness does not appear to be dimmed by the haze's gray pallor.

NASA image courtesy Jeff Schmaltz, MODIS Rapid Response Team, Goddard Space Flight Center





Scientist: Weather Was ‘Schizophrenic’ in 2004, December 30; *La Canada Valley Sun*; **Bill Patzert** (NASA JPL) interviewed by Jake Armstrong about wild weather in 2004.

December Rains and the Ongoing Drought, December 30; *KABC-Radio, Los Angeles*; **Bill Patzert** (NASA JPL) interviewed by Russ Spears about whether late December rains will improve California’s drought. Interview was also broadcast on other radio stations, including K-EARTH, 101.1 FM.

Indonesian Tsunami, December 27; *KABC-TV, Los Angeles*; **Bill Patzert** (NASA JPL) interviewed by Gene Gleeson for a story about the December 26 Indonesian tsunami and the likelihood of a similar event impacting California.

NASA Finds Polluted Clouds Hold Less Moisture and Cool Earth Less, December 23; *Nature.com, Science Blog*; A NASA study, conducted by **Andrew Ackerman** (NASA Ames), Michael Kirkpatrick (University of Tasmania, Hobart, Australia), David Stevens (Lawrence Livermore National Laboratory, Livermore, CA), and O. Brian Toon (University of Colorado, Boulder) finds some clouds that form on tiny haze particles are not cooling the Earth as much as previously thought.

NASA Investigator Honored, December 17; *Space Today*; **William Krabill** of NASA’s Wallops Flight Facility has won the William T. Pecora Award for excellence in remote sensing.

NASA Study Finds Tiny Particles in Air May Influence Carbon Sinks, December 16; *United Press International, Science Daily*; A NASA-funded study led by **Dev Niyogi** (North Carolina State University) provides direct measurements confirming aerosols, tiny particles in the atmosphere, may be changing how much carbon plants and ecosystems absorb from, or release to, the air.

NASA Scientists Discuss Giant Atmospheric Brown Cloud, December 15; *Christian Science Monitor, Science Daily*; NASA scientists announce a giant, smoggy atmospheric brown cloud, which forms over South Asia and the Indian Ocean, has intercontinental reach, according to **Robert Chatfield** (NASA Ames).

Greenland’s Ice Thinning More Rapidly at Edges, December 15; *United Press International*; **Waleed Abdalati** (NASA GSFC) and **William Krabill** (NASA Wallops) find that ice thinned along Greenland’s coastlines between 1997 and 2003 much more substantially than it had in the past.

NASA Eyes Ice Changes Around Earth’s Frozen Caps, December 14; *Washington Times, Science Blog*; NASA scientists **Waleed Abdalati** (NASA GSFC) and **William Krabill** (NASA Wallops) present findings on dramatic changes to Arctic sea ice and warming, glacier acceleration, and newly discovered relationships between ice sheets, sea-level rise, and climate warming

Aura Sheds New Light on Pollution, December 14; *ABC News, CNN, Washington Post*; NASA scientists announce the agency’s Aura spacecraft program, headed by **Phi DeCola** (NASA HQ) and **Mark Schoeberl** (NASA GSFC) is providing the first daily, direct global measurements of low-level ozone and many other pollutants affecting air quality.

NASA Finds Trees and Insect Outbreaks Affect Carbon Dioxide Levels, December 13; *Space Daily, New Scientist*; Insect control and tree planting could greatly affect Earth’s greenhouse gases, according to scientists **Christopher Potter** (NASA Ames), Pang-Ning Tan (Michigan State University, East Lansing) and Vipin Kumar (University of Minnesota, Minneapolis).

NASA’s ICESat Satellite Sees Changing World Affecting Many, December 13; *Chicago Chronicle, Houston Mirror*; NASA’s Ice, Cloud, and land Elevation Satellite’s (ICESat) precise measurements of Earth’s ice sheets, atmosphere, land masses, and volcanoes provide a unique look at our planet, according to **David Harding** (NASA GSFC)

Not the Usual Suspects: Profiles of the People Who Are Putting a New Face On Water Issues, December; *Aqueduct Magazine*; **Bill Patzert** (NASA JPL) profiled in the Metropolitan Water District

of Southern California's magazine, *Aqueduct*, highlighting that those not normally considered water experts can have a very profound influence on policy.

NASA Satellites Witnessed El Niño Creep in from the Indian Ocean, December 1; *WNCT-TV Channel 9, Greenville, NC, Science Daily*; Scott Curtis (East Carolina University, Greenville, N.C.) and **Robert Adler, George Huffman** and **Guojun Gu** (NASA GSFC) create a new index using satellite rain and wind data to see the development of El Niño events by looking at the Indian Ocean.

Study Finds Glacier Doing Double Time, December 1; *United Press International, Environment News Service*; A NASA-funded study led by **Waleed Abdalati** (NASA GSFC) used data from satellites and airborne lasers to derive ice movements and finds some glaciers have thinned by over a meter a year.

NASA Satellite Data to Aid Global Conservation, November 18; *Associated Press, Reuters*; NASA and The World Conservation Union, the world's largest environmental knowledge network, signed a joint declaration to use NASA satellite data to help in worldwide conservation efforts, reinforcing NASA's vision to use its "unique vantage from space" to improve life here on Earth, says **Ghassem Asrar** (NASA HQ)

NASA Research Shows Wetland Changes Affect Florida Freezes, November 18; *Scripps Howard, Knoxville News Sentinel*; The study, authored by Curtis Marshall and Roger Pielke (Colorado State University) and **Louis Steyaert** (USGS and NASA GSFC), finds a link between the losses of wetlands and more severe freezes in some agricultural areas of south Florida.

NASA Climatologists Named in Scientific American Top 50 Scientists, November 9; *SpaceRef*; NASA Climatologists, **Drew Shindell** and **Gavin Schmidt** (both NASA GISS), received the annual award given by Scientific American Magazine.

TRMM Satellite Proves El Niño Holds the Reins on Global Rains, November 8; *Science Daily, Innovations Report*; **Ziad Haddad** and **Jonathan Meagher** (both NASA JPL) and **Robert Adler** and **Eric Smith** (both NASA GSFC) find the El Niño Southern Oscillation is the main driver of the change in rain patterns all around the world.

Scientists Find Acid Rain An Unlikely Ally In The Battle Against A Greenhouse Gas, November 5; *Science Daily*; Vincent Gauci (Open University, United Kingdom) and **Elaine Matthews** (NASA GISS) discover that acid rain inhibits a swampland bacteria from producing methane, a greenhouse gas.

NASA and Partners Create New Worldwide Coral Reef Library, November 4; *Space Daily*; **Julie A. Robinson** (NASA JSC), Frank Muller-Karger (University of South Florida), and **Gene Carl Feldman** (NASA GSFC) discuss a new NASA-funded archive of some 1,500 images of worldwide coral reefs.



EOS Science Calendar

2005

May 24-27

AVIRIS Science Workshop, Pasadena, CA. Contact Robert O. Green, rog@jpl.nasa.gov. URL: aviris.jpl.nasa.gov

September 14-16

SORCE Team Meeting, Southwest, CO. Contact: Vanessa George, george@lasp.colorado.edu

Global Change Calendar

2005

April 24-29, 2005

European Geosciences Union General Assembly 2005, Vienna, Austria. URL: www.copernicus.org/EGU/ga/egu05/programme_overview.html

May 23-27, 2005

2005 AGU Joint Assembly, New Orleans, URL: www.agu.org/meetings/sm05/

June 20-24

5th International Scientific Conference on the Global Energy & Water Cycle, Orange County, CA. URL: www.gewex.org/5thconf.htm

June 20-24

31st International Symposium on Remote Sensing of Environment, "Global Monitoring for Sustainability and Security," Saint Petersburg, Russia. Call for Papers. URL: www.niersc.spb.ru/isrse/call_for_papers.shtml

July 25-29, 2005

IGARSS 25th Anniversary, Seoul, Korea. URL: www.igarss05.org/



Code 900
National Aeronautics and
Space Administration

Goddard Space Flight Center
Greenbelt, Maryland 20771

PRSRT STD
Postage and Fees Paid
National Aeronautics and
Space Administration
Permit G27

Official Business
Penalty For Private Use, \$300.00

The Earth Observer

The Earth Observer is published by the EOS Project Science Office, Code 900, NASA Goddard Space Flight Center, Greenbelt, Maryland 20771, telephone (301) 614-5561, FAX (301) 614-6530, and is available on the World Wide Web at eos.nasa.gov/earth_observer.php or by writing to the above address. Articles, contributions to the meeting calendar, and suggestions are welcomed. Contributions to the calendars should contain location, person to contact, telephone number, and e-mail address. To subscribe to *The Earth Observer*, or to change your mailing address, please call Hannelore Parrish at (301) 867-2114, or send a message to hannelore_parrish@ssaihq.com, or write to the address above.

The Earth Observer Staff:

Executive Editor: Steven Graham (steven.m.graham.2@gsfc.nasa.gov)

Technical Editors: Renny Greenstone (rennygr@earthlink.net)

Tim Suttles (4suttles@bellsouth.net)

Alan Ward (alan_ward@ssaihq.com)

Design and Production: Alex McClung (alexander_mcclung@ssaihq.com)

Distribution: Hannelore Parrish (hannelore_parrish@ssaihq.com)



Printed on Recycled Paper